Ore Geology Reviews 104 (2019) 208–226

Contents lists available at ScienceDirect

Ore Geology Reviews

journal homepage: www.elsevier.com/locate/oregeorev

Tectonic evolution and copper-gold metallogenesis of the Papua New Guinea and Solomon Islands region

Robert J. Holm[a,b,*], Simon Tapster[c,d], Hielke A. Jelsma[e], Gideon Rosenbaum[f], Darren F. Mark[g,h]

[a] Frogtech Geoscience, 2 King Street, Deakin West, ACT 2600, Australia
[b] Economic Geology Research Centre (EGRU), James Cook University, Townsville, Queensland 4811, Australia
[c] NERC Isotope Geosciences Laboratory, British Geological Survey, Nottingham NG12 5GG, UK
[d] Department of Geology, University of Leicester, Leicester LE1 7RH, UK
[e] Anglo American Exploration, P. O. Box 61587, Marshalltown 2107, South Africa
[f] School of Earth and Environmental Sciences, The University of Queensland, Brisbane, Queensland 4072, Australia
[g] Isotope Geoscience Unit, Scottish Universities Environmental Research Centre (SUERC), Rankine Avenue, East Kilbride, Scotland G75 0QF, UK
[h] Department of Earth & Environmental Science, School of Geography & Geosciences, University of St Andrews, St Andrews KY16 9AJ, UK

ARTICLE INFO

Keywords:
Papua New Guinea
Solomon Islands
Copper
Gold
Metallogenesis
Tectonic reconstruction

ABSTRACT

Papua New Guinea and the Solomon Islands are in one of the most prospective regions for intrusion-related mineral deposits. However, because of the tectonic complexity of the region and the lack of comprehensive regional geological datasets, the link between mineralization and the regional-scale geodynamic framework has not been understood. Here we present a new model for the metallogenesis of the region based on a synthesis of recent studies on the petrogenesis of magmatic arcs and the history of subduction zones throughout the region, combined with the spatio-temporal distribution of intrusion-related mineral deposits, and six new deposit ages. Convergence at the Pacific-Australia plate boundary was accommodated, from at least 45 Ma, by subduction at the Melanesian trench, with related Melanesian arc magmatism. The arrival of the Ontong Java Plateau at the trench at ca. 26 Ma resulted in cessation of subduction, immediately followed by formation of Cu-Au porphyry-epithermal deposits (at 24–20 Ma) throughout the Melanesian arc. Late Oligocene to early Miocene tectonic reorganization led to initiation of subduction at the Pocklington trough, and onset of magmatism in the Maramuni arc. The arrival of the Australian continent at the Pocklington trough by 12 Ma resulted in continental collision and ore deposit formation (from 12 to 6 Ma). This is represented by Cu-Au porphyry deposits in the New Guinea Orogen, and epithermal Au systems in the Papuan Peninsula. From 6 Ma, crustal delamination in Papua New Guinea, related to the prior Pocklington trough subduction resulted in adiabatic mantle melting with emplacement of diverse Cu and Au porphyry and epithermal deposits within the Papuan Fold and Thrust Belt and Papuan Peninsula from 6 Ma to the present day. Subduction at the New Britain and San Cristobal trenches from ca. 10 Ma resulted in an escalation in tectonic complexity and the onset of microplate tectonics in eastern Papua New Guinea and the Solomon Islands. This is reflected in the formation of diverse and discrete geodynamic settings for mineralization within the recent to modern arc setting, primarily related to upper plate shortening and extension and the spatial relationship to structures within the subducting slab.

1. Introduction

The region of Papua New Guinea and Solomon Islands hosts an abundance of porphyry, epithermal and skarn mineral deposits, such as Ok Tedi, Frieda River, Porgera, Wafi-Golpu, Ladolam (Lihir) and Panguna (Bougainville; Fig. 1; Cooke et al., 2005; Sillitoe, 2010; Richards, 2013). Globally, such mineral-systems account for approximately one-fifth of the world's gold (Au) and nearly three-quarters of the world's copper (Cu) resources (Cooke et al., 2005; Sillitoe, 2010). Formation of these types of deposits is considered to be genetically linked to intermediate to felsic intrusive arc magmatism, typified by regions such as the North American Cordillera, the Andean margin of South America and the Tethyan Belt of Eurasia (e.g. Cooke et al., 2005; Sillitoe, 2010; Richards, 2013; Richards and Holm, 2013; Butterworth et al., 2016). The general relationship between porphyry-epithermal mineralization and subduction zones across the globe implies that there are broad, plate margin-scale tectono-magmatic controls on where and when these deposits form in the crust (e.g. Richards, 2003; Cooke et al.,

* Corresponding author at: Frogtech Geoscience, 2 King Street, Deakin West, ACT 2600, Australia.
E-mail address: rholm@frogtech.com.au (R.J. Holm).

https://doi.org/10.1016/j.oregeorev.2018.11.007
Received 14 October 2017; Received in revised form 4 November 2018; Accepted 8 November 2018
Available online 10 November 2018
0169-1368/

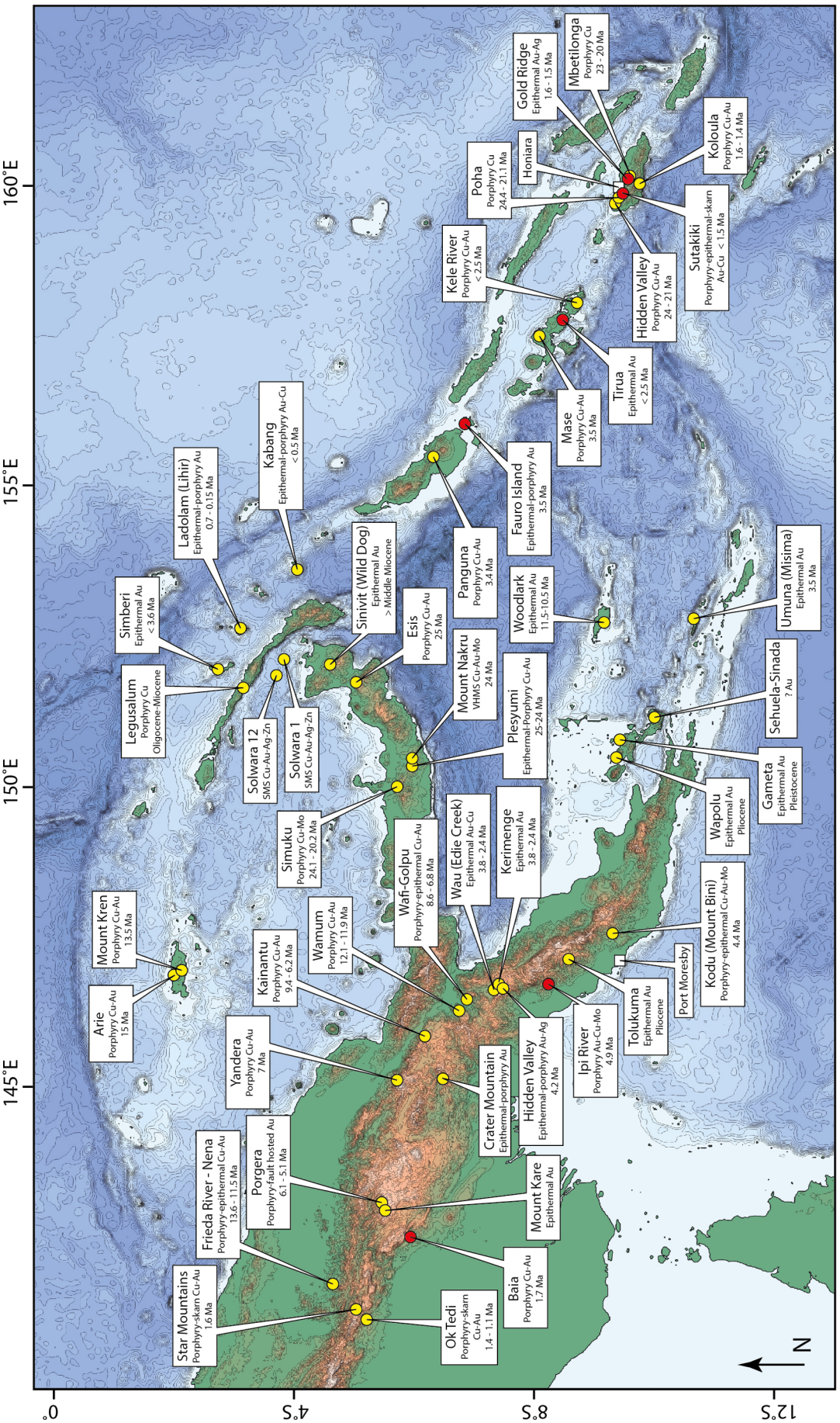

Fig. 1. Mineral deposits of the Papua New Guinea and Solomon Islands region. Red points indicate deposits and prospects host to samples dated in this study. (For interpretation of the references to colour in this figure legend, the reader is referred to the web version of this article.)

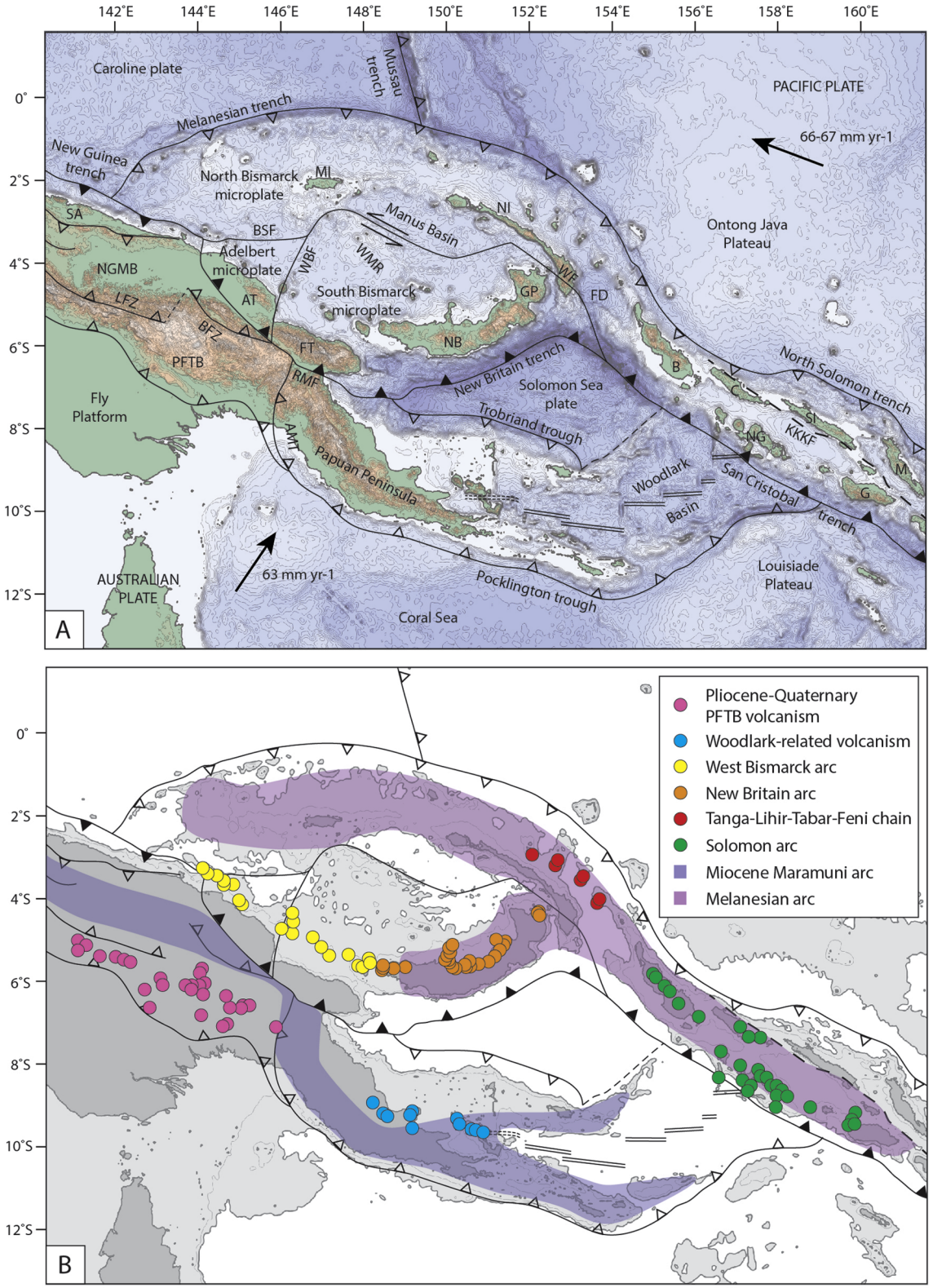

Fig. 2. Tectonic setting of Papua New Guinea and Solomon Islands. A) Regional plate boundaries and tectonic elements. Light grey shading illustrates bathymetry < 2000 m below sea level indicative of continental or arc crust, and oceanic plateaus. The New Guinea Orogen comprises rocks of the New Guinea Mobile Belt and the Papuan Fold and Thrust Belt; Adelbert Terrane (AT); Aure-Moresby trough (AMT); Bougainville Island (B); Bismarck Sea fault (BSF); Bundi fault zone (BFZ); Choiseul Island (C); Feni Deep (FD); Finisterre Terrane (FT); Guadalcanal Island (G); Gazelle Peninsula (GP); Kia-Kaipito-Korigole fault zone (KKKF); Lagaip fault zone (LFZ); Malaita Island (M); Manus Island (MI); New Britain (NB); New Georgia Islands (NG); New Guinea Mobile Belt (NGMB); New Ireland (NI); Papuan Fold and Thrust Belt (PFTB); Ramu-Markham fault (RMF); Santa Isabel Island (SI); Sepik arc (SA); Weitin Fault (WF); West Bismarck fault (WBF); Willaumez-Manus Rise (WMR). Arrows indicate rate and direction of plate motion of the Australian and Pacific plates (MORVEL, DeMets et al., 2010); B) Pliocene-Quaternary volcanic centres and magmatic arcs related to this study. Figure modified from Holm et al. (2016). Subduction zone symbols with filled pattern denote active subduction; empty symbols denote extinct subduction zone or negligible convergence.

2005). In particular, changes in the subduction regime are commonly considered as crucial parameters triggering mineralizing events, for example, associated with terrane collisions, subduction of slab structure (e.g., aseismic ridge), or changes in the slab angle during subduction (Cooke et al., 2005; Rosenbaum et al., 2005; Sillitoe, 2010; Rosenbaum and Mo, 2011; Richards, 2013; Richards and Holm, 2013). A detailed understanding of the geological settings linked to deposit emplacement is required when mineral exploration progresses to target concealed deposits beneath cover. This needs to be applied at all scales, but we draw particular attention to the need for an appreciation of regional tectonics and the inherent tectonic complexities that arise through time that may be favorable for deposit emplacement.

The present-day geodynamic setting of Papua New Guinea and the Solomon Islands is a complex zone of oblique convergence at the boundary between the Australian and Pacific plates, trapped between the converging Ontong Java Plateau and Australian continent (Fig. 2). The general tectonic framework of the southwest Pacific has been discussed in previous studies (e.g. Hall, 2002; Schellart et al., 2006), but there are still major uncertainties regarding the complex geodynamics of Papua New Guinea and Solomon Islands (e.g. Hall, 2002; Holm et al., 2016). In addition, current geological and ore deposit datasets for this area are inadequate to inform meaningful conclusions. This study takes a high-level approach to this problem by addressing metallogenesis in terms of regional metal endowment and mineralization-styles rather than emphasizing the details of individual deposits or ore system-scale mechanisms for generation of mineral concentrations.

Recent work investigating the petrogenesis of magmatic arcs throughout the Papua New Guinea and Solomon Islands region (Schuth et al., 2009; Woodhead et al., 2010; Holm and Richards, 2013; Holm et al., 2013, 2015b), combined with regional plate tectonic modelling (Holm et al., 2016), provide a framework for us to develop a regional metallogenic model. In this study we build on the preliminary work of Holm et al. (2015a) to test the hypothesis that subduction-related ore deposits have formed under special circumstances, for example, related to terrane collision, ridge subduction or slab tearing. To achieve this, we combine information on subduction processes and arc magmatism with the distribution of mineral deposits, the styles of mineralization, and the timing of mineralization. We also present new age dates on deposits and prospects. This allows us to provide a more comprehensive regional model for the formation of intrusion-related porphyry and epithermal deposits in the Papua New Guinea and Solomon Islands region through time, with implications for future exploration strategies.

2. Tectonic setting

The Papua New Guinea mainland is composed of multiple terranes that were accreted to the northern Australian continental margin during the Cenozoic (e.g. Hill and Hall 2003; Crowhurst et al., 2004; Davies, 2012; Holm et al., 2015b). The result is an accretionary orogen characterized by sedimentary cover rocks on Australian continental crust (Papuan Fold and Thrust Belt; Dow, 1977; Hill and Gleadow, 1989; Craig and Warvakai, 2009), which is buttressed against variably deformed sedimentary, metamorphic and crystalline rocks of the composite New Guinea Mobile Belt (Fig. 2; Dow et al., 1972; Dow, 1977; Hutchison and Norvick, 1980; Hill and Raza, 1999; Davies, 2012). Together the Papuan Fold and Thrust Belt and the New Guinea Mobile Belt comprise the New Guinea Orogen. In contrast, the islands of eastern Papua New Guinea and the Solomon Islands represent island arc terranes formed adjacent to the Australia-Pacific plate boundary (Abbott, 1995; Hall, 2002; Lindley, 2006; Holm et al., 2016). More detailed reviews of the regional tectonics can be found in Baldwin et al. (2012) and Holm et al. (2016), and references therein.

To the east of Papua New Guinea, plate convergence is currently accommodated by subduction of the Australian and Solomon Sea plates at the San Cristobal and New Britain trenches, respectively (Fig. 2). Magmatism associated with these subduction zones occurs in the Solomon arc, the Tanga-Lihir-Tabar-Feni chain and the New Britain arc, overprinting Melanesian arc basement related to earlier subduction at the Melanesian trench (Woodhead et al., 1998; Petterson et al., 1999; Holm et al., 2013). The western extension of the New Britain trench and New Britain arc are the north-dipping Ramu-Markham fault zone, and the West Bismarck arc, respectively (Fig. 2; Abbott, 1995; Woodhead et al., 2010; Holm and Richards, 2013).

Active rifting and seafloor spreading occur in the Bismarck Sea back-arc basin, which comprises the North Bismarck and South Bismarck microplates, separated by the left-lateral strike-slip Bismarck Sea fault (Fig. 2; Denham 1969; Taylor 1979; Cooper and Taylor, 1987; Holm et al., 2016). The Woodlark Basin is an active extensional basin (Fig. 2) that began rifting at ca. 6 Ma (Taylor et al., 1995, 1999; Holm et al., 2016). To the west of the Woodlark Basin oceanic spreading gradually transitions to continental rifting of the Papuan Peninsula (Benes et al., 1994; Taylor et al., 1995, 1999). Young oceanic crust, including the active Woodlark spreading center, are currently subducting to the northeast at the San Cristobal trench (Mann et al., 1998; Chadwick et al., 2009; Schuth et al., 2009).

The Papua New Guinea and Solomon Islands region also preserves several subduction zones that are either extinct or accommodate only minor convergence at the present day. The Melanesian trench accommodated southwest-dipping subduction of the Pacific plate beneath the Australian plate and is associated with magmatism of the Melanesian arc (Petterson et al., 1999; Hall, 2002; Schellart et al., 2006; Holm et al., 2013). The location and orientation of subduction beneath the Papua New Guinea mainland that gave rise to the early to late Miocene Maramuni arc (Dow, 1977; Weiland, 1999), is by comparison a more contentious element of the regional tectonics (see Hall and Spakman, 2002; Holm et al., 2015b; Holm et al., 2016, and references therein). Here, we adopt the model that suggests that subduction at the Pocklington trough (and the westward extension thereof into Papua New Guinea) gave rise to tectono-magmatic phenomena within Papua New Guinea and the Maramuni arc (e.g. Dow, 1977; Webb et al., 2014; Holm et al., 2015b). An alternative model invoking subduction at the Trobriand trough will be discussed below. At present, the Pocklington trough marks the southern margin of the Woodlark Basin. The interpreted western extension of this structure includes the Aure-Moresby trough southwest of the Papuan Peninsula (e.g. Ott and Mann, 2015), which forms a suture between the Papuan Fold and Thrust Belt and the New Guinea Mobile Belt (Fig. 2; e.g. Dow et al., 1972; Dow, 1977; Holm et al., 2015b). This proto-Pocklington trough is considered to represent a relict trench that accommodated north-dipping subduction of the Australian plate beneath New Guinea (Hill and Hall, 2003; Cloos et al., 2005; Webb et al., 2014; Holm et al., 2015b), but may accommodate some recent convergence (e.g. Ott and Mann, 2015). The Trobriand trough marks the southern margin of the Solomon Sea (Fig. 2), which according to plate reconstructions (Holm et al., 2016), was an active subduction zone during the Pliocene (but not in the Miocene). No arc magmatism has been attributed to subduction at the Trobriand trough.

3. Mineral deposits

Research on mineral deposits in the Papua New Guinea and Solomon Islands region has been mainly focused on the nature and controls of individual deposits and their district-scale setting (e.g. Richards and Ledlie, 1993; Hill et al., 2002; Gow and Walshe, 2005; Tapster et al., 2016). To investigate relationships between the evolution of the subduction arcs and the metallogenesis of intrusion-related mineral deposits, we used data available from 47 Cenozoic intrusion-related Cu-Au deposits (Table 1; Figs. 1 and 3), encompassing active mines, deposits and prospects. Our dataset has information on deposit style and the total deposit endowment, including deposit tonnage, and copper and gold grades (Fig. 3). Metal endowment for each deposit was calculated based on deposit tonnage and metal grade. Data were sourced from recent company reports where possible, and were

Table 1
Mineral deposit resource and age data.

Deposit	Scale	Country	Long.	Lat.	Tectonic Province	Deposit Type	Resource	Total Tonnage (Mt)	Au Grade (g/t)	Au Tonnage (Moz)	Cu Grade (%)	Cu Tonnage (Mt)	Age (Ma)	Dating Method	Age for plot (Ma)	Age Reference
Gold Ridge	Mine	Solomon Islands	160.14	−9.58	Island Arcs	Epithermal	Au-Ag	64.2	1.5	3.4			1.6–1.5	Ar-Ar (Adl)	0–3	This study
Hidden Valley (PNG)	Mine	PNG	146.67	−7.46	NGO	Epithermal-porphyry	Au-Ag	42	1.6	2.4			4.2	K-Ar (Adl)	3–6	Nelson et al., 1990
Kainantu	Mine	PNG	145.86	−6.20	NGO	Porphyry	Cu-Au	5.5	7.2	1.4	1.8	0.1	9.4–6.2	U-Pb (zircon)	6–9	Holm et al., 2015
Ladolam (Lihir)	Mine	PNG	152.63	−3.13	Island Arcs	Epithermal-porphyry	Au	820	2.2	63.6			0.7–0.15	K-Ar (WR Bt Ilt Kfs)	0–3	Moyle et al., 1990
Ok Tedi	Mine	PNG	141.14	−5.21	NGO	Porphyry-skarn	Cu-Au	911	0.52	16.7	0.43	3.9	1.4–1.1	U-Pb (zircon)	0–3	van Dongen et al., 2010b
Panguna	Mine	PNG	155.50	−6.33	Island Arcs	Porphyry	Cu-Au	1838	0.34	22.0	0.3	5.5	3.4	K-Ar (WR Bt Kfs Pl)	3–6	Page and McDougall, 1972a
Porgera	Mine	PNG	143.08	−5.46	NGO	Porphyry	Au	68.2	4.4	10.6			6.1–5.1	Ar-Ar (Bt Hbl)	3–6	Richards and McDougall, 1990
Simberi	Mine	PNG	151.97	−2.75	Island Arcs	Epithermal	Au	120.9	1.3	5.5			3.6–1.9	K-Ar (WR Alu Pl) Ar-Ar (Amp Cpx)	0–3	McInnes, 1992; Rytuba et al., 1993
Sinivit (Wild Dog)	Mine	PNG	152.05	−4.61	Island Arcs	Epithermal	Au	0.96	5.83	0.2			> Middle Miocene	Stratigraphic	21–24	Lindley, 1990
Tolukuma	Mine	PNG	147.13	−8.56	NGO	Epithermal	Au	0.3	29.9	0.3			Pliocene	K-Ar (WR?)	3–6	Langmead and McLeod, 1990
Umuna (Misima)	Mine	PNG	152.81	−10.66	NGO	Epithermal	Au	43	1.1	1.7			4.0–3.2	K-Ar (Ser) Ar-Ar (Ser)	3–6	Adshead, 1997
Woodlark	Mine	PNG	152.72	−9.19	NGO	Epithermal	Au	45.1	1.5	2.4			11.5–10.5		9–12	Burkett et al., 2015
Arie	Deposit	PNG	146.88	−2.02	Island Arcs	Porphyry	Cu-Au	165			0.32	0.5	15	K-Ar	12–15	Singer et al., 2008
Crater Mountain	Deposit	PNG	145.17	−6.49	NGO	Epithermal-porphyry	Au	24	1.0	0.8					0–3	
Frieda River	Deposit (Feasibility)	PNG	141.73	−4.66	NGO	Porphyry	Cu-Au	2777	0.23	22.5	0.47	13.1	13.6–11.5	K-Ar (Bt Hbl Pl Ser)	9–12	Whalen et al., 1982
Gameta	Deposit	PNG	150.79	−9.42	NGO	Epithermal	Au	5.1	1.8	0.3			Pleistocene		0–3	Chapple and Ibil, 1998; Garwin et al., 2005
Kabang (Feni Island)	Deposit	PNG	153.61	−4.09	Island Arcs	Epithermal-porphyry	Au-Cu	19.9	1.01	0.7			< 0.5	K-Ar	0-3	Sillitoe, 1989; Garwin et al., 2005
Kerimenge	Deposit	PNG	146.72	−7.42	NGO	Epithermal	Au	55	1	1.9			3.8–2.4	K-Ar (Bt Pl)	3–6	Hutton et al., 1990; Page and McDougall, 1972b
Kodu (Mount Bini)	Deposit	PNG	147.58	−9.30	NGO	Porphyry-epithermal	Cu-Au-Mo	276	0.3	2.9	0.27	0.7	4.4		3–6	Dugmore and Leaman, 1998; Garwin et al., 2005
Koloula	Deposit	Solomon Islands	160.03	−9.78	Island Arcs	Porphyry	Cu-Au	50			0.17	0.1	1.6–1.4	U-Pb (zircon)	0–3	Tapster et al., 2016

(*continued on next page*)

Table 1 (*continued*)

Deposit	Scale	Country	Long.	Lat.	Tectonic Province	Deposit Type	Resource	Total Tonnage (Mt)	Au Grade (g/t)	Au Tonnage (Moz)	Cu Grade (%)	Cu Tonnage (Mt)	Age (Ma)	Dating Method	Age for plot (Ma)	Age Reference
Legusalum	Deposit	PNG	151.65	−3.18	Island Arcs	Porphyry	Cu						Oligocene-Miocene		21–24	Singer et al., 2008
Mbetilonga	Deposit	Solomon Islands	160.16	−9.61	Island Arcs	Porphyry	Cu						23–20		21–24	Hackman, 1980
Mount Kare	Deposit	PNG	142.97	−5.54	NGO	Epithermal	Au	42.5	1.54	2.3					3–6	Inferred from Porgera
Mount Kren	Deposit	PNG	146.94	−2.16	Island Arcs	Porphyry	Cu-Au						13.5	K-Ar	12–15	Singer et al., 2008
Mount Nakru	Deposit	PNG	150.47	−5.97	Island Arcs	VHMS	Cu-Au-Mo	38.4	0.28	0.4	0.61	0.2	24	K-Ar	21–24	Singer et al., 2008
Nena	Deposit	PNG	141.73	−4.65	NGO	Epithermal	Cu-Au	45	0.6	1.0	2.55	1.1	13.6–11.5	K-Ar (Bt Hbl Pl Ser)	9–12	Hall et al., 1990; Whalen et al., 1982
Plesyumi	Deposit	PNG	150.38	−5.97	Island Arcs	Epithermal-porphyry	Cu-Au						25–24	K-Ar	24–27	Titley, 1978; Garwin et al., 2005
Sehuela-Sinada	Deposit	PNG	151.16	−9.99	NGO		Au	10	0.5	0.2						
Simuku	Deposit	PNG	150.02	−5.72	Island Arcs	Porphyry	Cu-Mo	200	0.06	0.4	0.36	0.7	24.1–20.2	U-Pb (zircon)	21–24	Holm et al., 2013
Solwara 1	Deposit	PNG	152.10	−3.79	Island Arcs	SMS	Cu-Au-Ag-Zn	2.6	5.9	0.5	7.7	0.2			0–3	
Solwara 12	Deposit	PNG	151.88	−3.71	Island Arcs	SMS	Cu-Au-Ag-Zn	0.23	3.6	0.03	7.3	0.02			0–3	
Star Mountains (Futik)	Deposit	PNG	141.33	−5.07	NGO	Porphyry-skarn	Cu-Au	65	0.1	0.2	0.54	0.4	1.6	K-Ar	0–3	Arnold and Griffin, 1978; Garwin et al., 2005
Wafi-Golpu	Deposit (Feasibility)	PNG	146.45	−6.88	NGO	Porphyry-epithermal	Cu-Au	996	0.83	29.2	0.83	8.3	8.6–6.8	Ar-Ar (Bt)	6–9	Lunge Bawasu, 2013
Wapolu	Deposit	PNG	150.50	−9.36	NGO	Epithermal	Au	2	2.4	0.2			Pliocene		3–6	McNeil, 1990
Wau (Edie Creek)	Deposit	PNG	146.66	−7.36	NGO	Epithermal	Au-Cu	7.5	3.7	1.0			3.8–2.4	K-Ar (Bt Pl)	3–6	Carswell, 1990; Page and McDougall, 1972b
Yandera	Deposit	PNG	145.13	−5.74	NGO	Porphyry	Cu-Au	747	0.061	1.6	0.33	2.5	7	K-Ar	6–9	Singer et al., 2008
Baia	Prospect	PNG	142.53	−5.95	NGO	Porphyry	Cu-Au						1.7	U-Pb (zircon)	0–3	This study
Esis	Prospect	PNG	151.74	−5.04	Island Arcs	Porphyry	Cu-Au						25	K-Ar	24–27	Hine et al., 1978; Garwin et al., 2005
Fauro Island	Prospect	Solomon Islands	156.04	−6.84	Island Arcs	Epithermal-porphyry	Au						3.5	U-Pb (zircon)	3–6	This study
Hidden Valley (Solomon)	Prospect	Solomon Islands	159.73	−9.37	Island Arcs	Porphyry	Cu-Au						24–21	K-Ar U-Pb (zircon)	21–24	Hackman, 1980; Tapster et al., 2014
Ipi River	Prospect	PNG	146.71	−8.25	NGO	Porphyry	Au-Cu-Mo						4.9	U-Pb (zircon)	3–6	This study
Kele River	Prospect	Solomon Islands	158.07	−8.75	Island Arcs	Porphyry	Cu-Au	1.5	1.8	0.1			< 2.5		0–3	Dunkley, 1986
Mase	Prospect	Solomon Islands	157.52	−8.08	Island Arcs	Porphyry	Cu-Au						3.5		3–6	Singer et al., 2008
Poha	Prospect	Solomon Islands	159.83	−9.43	Island Arcs	Porphyry	Cu						24.4–21	K-Ar (Hbl)	21–24	Chivas and McDougall, 1978

(*continued on next page*)

Table 1 (*continued*)

Deposit	Scale	Country	Long.	Lat.	Tectonic Province	Deposit Type	Resource	Total Tonnage (Mt)	Au Grade (g/t)	Au Tonnage (Moz)	Cu Grade (%)	Cu Tonnage (Mt)	Age (Ma)	Dating Method	Age for plot (Ma)	Age Reference
Sutakiki	Prospect	Solomon Islands	160.08	−9.69	Island Arcs	Porphyry-epithermal-skarn	Au-Cu						< 1.5	U-Pb (zircon)	0–3	This study
Tirua	Prospect	Solomon Islands	157.79	−8.47	Island Arcs	Epithermal	Au						< 2.5	U-Pb (zircon)	0–3	This study
Wamum	Prospect	PNG	146.28	−6.75	NGO	Porphyry	Cu-Au	45	0.12	0.2	0.3	0.1	12.1–11.9	U-Pb (zircon)	9–12	Holm et al., 2015

Total tonnage is given for combined reserve and resources.
Information regarding dated materials is not provided by Garwin et al. (2005) or Singer et al. (2008).
Abbreviations: PNG, Papua New Guinea; NGO, New Guinea Orogen; WR, whole rock; Adl, adularia; Alu alunite; Amp, amphibole; Bt, biotite; Cpx, clinopyroxene; Hbl, hornblende; Ilt, Illite; Kfs, K-feldspar; Pl, plagioclase; Ser, sericite.

supplemented by data from Garwin et al. (2005), Singer et al. (2008) and other relevant literature (see Table 1; reported deposit information is not intended as a JORC-compliant category; deposit endowment references are included in the supplementary material).

The geochronological dataset is supplemented by new radiometric constraints for six deposits. Additional constraints are based on field observations and stratigraphic relationships. Uncertainties within the dataset originate from both parametric sources (quoted uncertainty due to analysis and systematic uncertainties e.g. decay constants), and non-parametric geological uncertainty, for example, the difference between the dated igneous intrusion and the hydrothermal system or alteration episode.

Mineral deposits throughout the Papua New Guinea and Solomon Islands region range in age from late Oligocene to Quaternary (Table 1; Fig. 1). The age of copper and gold mineral deposits in mainland Papua New Guinea ranges from Miocene to Quaternary. These deposits are dominated by porphyry-type deposits, which formed within the New Guinea Orogen (e.g., Ok Tedi, Frieda River, Porgera, Wafi-Golpu; Fig. 1). Epithermal- and porphyry-type deposits, such as Hidden Valley (Papua New Guinea) and Tolukuma, occur along the Papuan Peninsula and extend east into the Woodlark Basin (Umuna, Misima Island and Woodlark deposits). Commodities throughout mainland Papua New Guinea vary between copper-rich and gold-rich deposits (Figs. 1 and 3). The islands in eastern Papua New Guinea and the Solomon Islands represent island arc settings with deposits ranging from Oligocene to recent ages. These deposits occur as porphyry- and epithermal-type deposits, as well as seafloor massive sulphide (SMS) deposits, with no clear trend in either copper or gold dominated systems (Figs. 1 and 3). Well-known deposits within this region are represented by the high-grade SMS Solwara deposits, and the giant Ladolam (Lihir) and Panguna (Bougainville) deposits.

4. Samples and methodology

4.1. Samples

Six rock samples were obtained from mines, deposits and prospects for the purpose of gaining new geochronological constraints on the timing of deposit formation. The chosen samples represent either recently discovered mineralized localities with no timing constraint or historically identified mineral occurrences that have lacked conclusive age dating.

Two samples (109472a and JD15) are from Papua New Guinea (see Fig. 1). Sample 109472a, from the Ipi River porphyry Cu-Au-Mo and epithermal Au prospect (146.71°E 8.25°S), is an intensely stockworked, altered and mineralized porphyritic andesite. The prospect is located in the Owen Stanley Ranges of the central Papuan Peninsula, approximately 50 km northwest of the Tolukuma mine. Sample JD15 (668956 9341950 UTM AGD66 zone 54S) is from the Baia porphyry Cu-Au prospect located southwest of Porgera within the Papuan Fold and Thrust Belt. The sample is a crystal-rich lapilli tuff of andesitic composition, with complexly zoned plagioclase and minor hornblende in a fine-grained fragmental matrix. Both samples are derived from magmatic occurrences associated with mineralization and represent the probable maximum age for mineralization.

Sample SI11886 (6°51′49.24″S 156° 5′9.73″E; Turner and Ridgeway, 1982), from Fauro Island in the Solomon Islands, is a porphyritic hornblende-biotite dacite from the calc-alkaline volcanic sequence that was emplaced into a late Oligocene-early Miocene tholeiitic lava sequence associated with earlier Melanesian arc growth (Turner and Ridgeway, 1982). A number of high-grade epithermal Au-Ag prospects are hosted by the dacitic volcanism and likely share a genetic association. The dacitic volcanism has not previously been dated by radio-isotopic methods and no biostratigraphic ages are available, but some authors have proposed a potentially pre-Pliocene age (Turner and Ridgway, 1982).

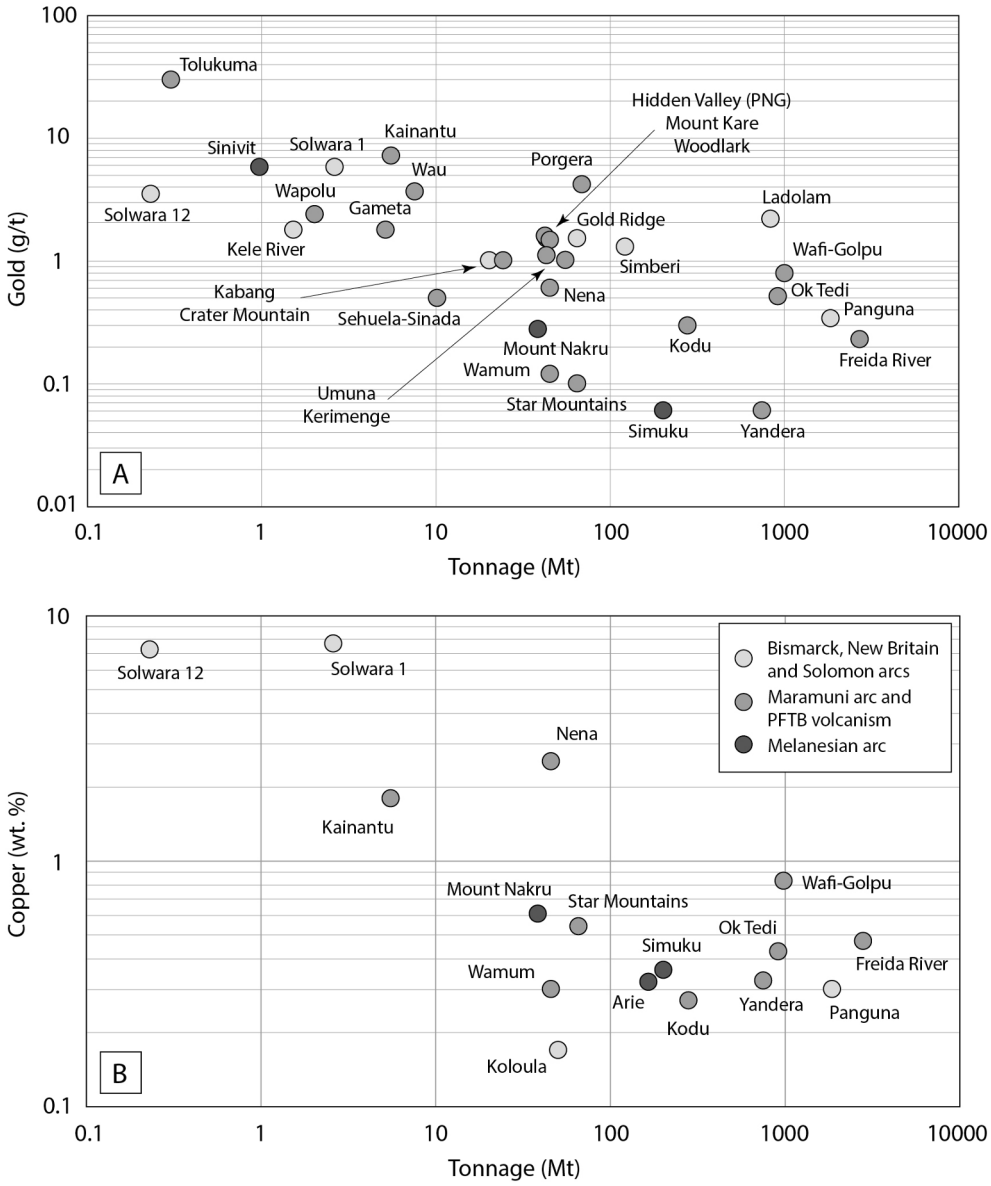

Fig. 3. Grade vs tonnage plots for A) gold and B) copper for mines, deposits and prospects with reported resources. Note logarithmic scale for metal grades and tonnage; data are listed in Table 1.

The Choe Intrusive complex of southeast New Georgia is host to the Tirua Hill prospect (also known as Hube River). The complex represents a nested sequence of picritic gabbro-microgranite intrusives (Dunkley, 1986) that was emplaced into an island arc picritic basalt volcanic sequence. This sequence represents the earliest stages of island growth linked to initial Woodlark spreading ridge subduction (Rohrbach et al., 2005) so the intrusion age represents a minimum constraint on the timing of this tectonic event. The Tirua Hill Prospect contains minor occurrences of secondary biotite in association with pervasive sericitic and silicic alteration, zones of argillic alteration and a large propylitic halo, in addition to (Au, Ag, Cu, Pb, Zn) sulfide and sulfosalt minerals (Dunkley, 1986). Sample SI1059 (8°28′6.42″S 157°47′53.63″E) is a diorite from this zone that postdates the pictritic magmatism and contains a stockwork of oxidized pyritic stringers, representing a maximum age for mineralization.

The Sutakiki prospect is located in central Guadalcanal and lies ~10 km north-northeast of the ca. 1.6–1.45 Ma plutonic Koloula Porphyry prospect (Tapster et al., 2016) and ~10 km south-southwest from the low-sulphidation epithermal Gold Ridge Mine, along the strike of an arc-normal structural corridor (Hackman, 1980; Swiridiuk, 1998, Tapster et al., 2011). The prospect is hosted by sheared ophiolitic mafic rocks and limestones and contains a range of high-grade Au epithermal and skarn mineralization and porphyry-style alteration, hosted by a porphyritic intrusion intersected within drill core. Sample SK001_346-346.27 m (9°41′26.37″S 160° 4′58.50″E) is a porphyritic hornblende diorite that has weak propylitic alteration and contains minor stringers of pyrite and chalcopyrite, with the age of intrusion taken to represent the maximum age for mineralization but with a close genetic association between magmatic and hydrothermal systems in the area.

Gold Ridge Mine, Guadalcanal is hosted by a supra-crustal volcaniclastic infill of a fault controlled rhombohedral basin that lies at the north-northeast extent of the arc-normal structural corridor that also contains the Sutakiki and Koloula Prospects (Hackman, 1980; Swiridiuk, 1998). The ore body contains Au, primarily hosted as native Au and electrum, found in association with chalcopyrite, galena, sphalerite, pyrite-marcasite, and arsenopyrite. Two samples, GDC3 279.45 and GDC5 45.8 (9°35′25.90″S, 160° 7′44.01″E), with quartz-adularia-carbonate-sulfide assemblages, probably reflecting the "stage-

1" 266–280 °C veins (Corbett and Leach, 1998) were selected for Ar-Ar dating of adularia from the upper and lower sections of the orebody that was intersected in recent (2013) drill holes in the Charivunga Gorge Extension.

4.2. U-Pb geochronology

U-Pb dating was conducted on magmatic zircon grains associated with intrusion-related deposits and prospects. Zircon grains were separated from hand samples or drill cores using standard techniques. They were then handpicked under a binocular microscope and imaged using cathodoluminescence (CL). Zircon U-Pb geochronology analyses for samples from Papua New Guinea were conducted at the Advanced Analytical Centre of James Cook University using a Coherent GeolasPro 193 nm ArF Excimer laser ablation system connected to a Bruker 820-ICP-MS (for methodology, see Holm et al. 2013, 2015b). Zircon grains from the Solomon Islands, with the exception of SI11886, were analyzed for U-Pb geochronology using a Nu Instruments Attom HR single-collector inductively coupled plasma mass spectrometer (HR-ICP-MS) with laser ablation performed by a New Wave Research UP193ss laser (NERC Isotope Geosciences Laboratories, British Geological Survey; see Tapster et al. 2014 for methodology). Sample SI11886 was analyzed using a Nu Plasma HR multi-collector ICP-MS, following the methods of Thomas et al. (2016). Further information on data collection, validation and reduction are provided in the supplementary materials.

4.3. Ar-Ar geochronology

Following sample screening and petrographic studies, Gold Ridge adularia was identified within < 2 cm composite veinlets, as < 500 μm-sized crystals that are inter-grown with quartz and carbonate minerals. The fine-grained nature of the target minerals and cm-scale vein size that was intercalated with wall rock material required development of a non-standard procedure to extract clean adularia separates for irradiation and Ar-Ar analyses. Samples were initially cut to remove as much of the host material adhered to the vein as possible, this was then leached in a warm bath of weak citric acid to reduce the calcite within the vein and aide disaggregation. The acid was frequently replaced until no effervescence occurred when the fresh acid was introduced. Following hand-crushing, sieving, washing, and electromagnetic separation, non-magnetic fractions 355–500 μm were passed through LST (lithium polytungstates) heavy liquids twice at the required densities to initially remove pyrite and then to remove quartz. The appropriate density fraction was then laid in a grid formation on carbon tape and examined under environmental mode SEM to screen the remaining grains; this was an important step as grains were commonly composite quartz-adularia, or had clear Na peaks, suggesting that the feldspar was likely to be derived from the feldspathic-altered wall rock material rather than primary hydrothermal adularia. The best grains were selected and removed from the carbon tape to form the mineral separate. Mineral separates were irradiated at the Cd-lined McMaster facility, Ontario, Canada, for 5 min after being packaged into Al-discs. J values were calculated via the irradiation of Alder Creek Sanadine (1.1891 ± 0.0006 Ma; Niespolo et al., 2016). Samples were analysed at Scottish Universities Environmental Research Council facility, East Kilbride. Full details on the analytical procedures are described in the supplementary information.

5. Geochronology results

Results for zircon U–Pb age dating for the selected samples from Ipi River, Baia, Fauro Island, Tirua and Sutakiki are shown in Fig. 4, and Ar-Ar adularia ages for Gold Ridge are shown in Fig. 5. These final interpreted ages are also included in Table 1. The results do not show evidence for significant isotopic disturbance or mixing of different age domains during zircon ablation, nor is there any significant difference in the age of zircon cores and rims. The complete zircon isotopic data can be found in the supplementary material.

All interpreted magmatic crystallization ages are Pliocene to Quaternary. Uncertainties are reported at a 2σ level with a minimum uncertainty reported at 0.1 Myr. Sample 109472a from Ipi River yielded a crystallization age of 4.9 ± 0.1 Ma (N = 14; MSWD = 1.4); sample JD15 from Baia returned an age of 1.70 ± 0.1 Ma (N = 24; MSWD = 1.4). The Tirua Hill sample SI1059 yielded an age of 2.4 ± 0.1 Ma (N = 20; MSWD = 1.1); the Fauro Island sample, SI11886, returned an age of 3.4 ± 0.2 Ma (N = 8; MSWD = 2.2); sample SK001_346-346.27 m from Sutakiki yielded an age of 1.54 ± 0.1 Ma (N = 10; MSWD = 1.4).

The two Adularia bearing vein samples from the Gold Ridge Mine yielded 100% plateau ages of 1.63 ± 0.05/0.06 Ma and 1.51 ± 0.09/0.09 Ma, (quoted at 1σ with the latter value including decay constant uncertainties) and are indistinguishable within uncertainty. Data precision is controlled by the large degree of atmospheric contamination.

6. Plate tectonic reconstructions

Plate tectonic reconstructions allow us to observe and test relationships between major tectonic events and the location and timing of mineral deposit formation. The reconstructions of this study build on the work by Holm et al. (2015a, 2016) but are extended back to 30 Ma to encompass the main regional ore-forming events. The plate tectonic reconstructions (Figs. 6–8) were developed using GPlates software (e.g. Boyden et al., 2011; Seton et al., 2012). Plate kinematics were resolved relative to the global moving hotspot reference frame (Müller et al., 2016) using the regional plate motion framework from prior reconstructions (Seton et al., 2012; Holm et al., 2016; Müller et al., 2016). The reconstructions (Figs. 6–8) are presented in relative reference frames for ease of visualization. These reconstructions were simplified and are mainly aimed at emphasizing major tectonic reorganization events associated with the evolution of the Melanesian arc, Maramuni arc, and New Britain and Solomon arcs. The plate features and rotation files for these reconstructions are available in the supplementary material. The development of detailed plate tectonic reconstructions for the region is beyond the scope of this study.

A range of datasets and models specific to the Papua New Guinea and Solomon Islands region were incorporated in the reconstructions (see Holm et al., 2016 for details). To extend the plate reconstructions back to 30 Ma, the previous dataset was expanded using constraints on the timing of major plate boundary events (e.g. Cloos et al., 2005; Knesel et al., 2008; Holm et al., 2015b). In this study we make the assumption that subduction of the Pacific plate was occurring at the Melanesian trench from ca. 45 Ma and all upper plates were fixed to the Australian plate motion. Collision of the Ontong Java Plateau with the Solomon Islands at ca. 26 Ma (Petterson et al., 1999; Knesel et al., 2008; Holm et al., 2013) terminated convergence between the Pacific plate and Solomon arc. This collision event, combined with contemporaneous arc-continent collision between the New Guinea Mobile Belt and Sepik Arc in the late Oligocene (not shown; Dow, 1977; Crowhurst et al., 1996), is interpreted to result in a shift of regional convergence to subduction at the Pocklington trough. At this time, the composite New Guinea Mobile Belt terrane and Solomon Sea became fixed to the Pacific plate motion. At ca. 12 Ma, collision of the Australian continent with the New Guinea Mobile Belt closed the Pocklington Sea, but subduction did not initiate at the New Britain-San Cristobal trench until ca. 10 Ma. Because of the limitations of rigid plate behavior we assume that 10 Ma was the timing of complete cessation of convergence at the Pocklington trough and initiation of subduction at the New Britain-San Cristobal trench. After 10 Ma, the New Guinea Mobile Belt and Solomon Sea plate motion were fixed to the Australian plate, until the onset of regional microplate tectonics from ca. 6 Ma (Holm et al. 2016).

The plate tectonic reconstructions were then correlated with the formation of mineral deposits in time and space. The timing and

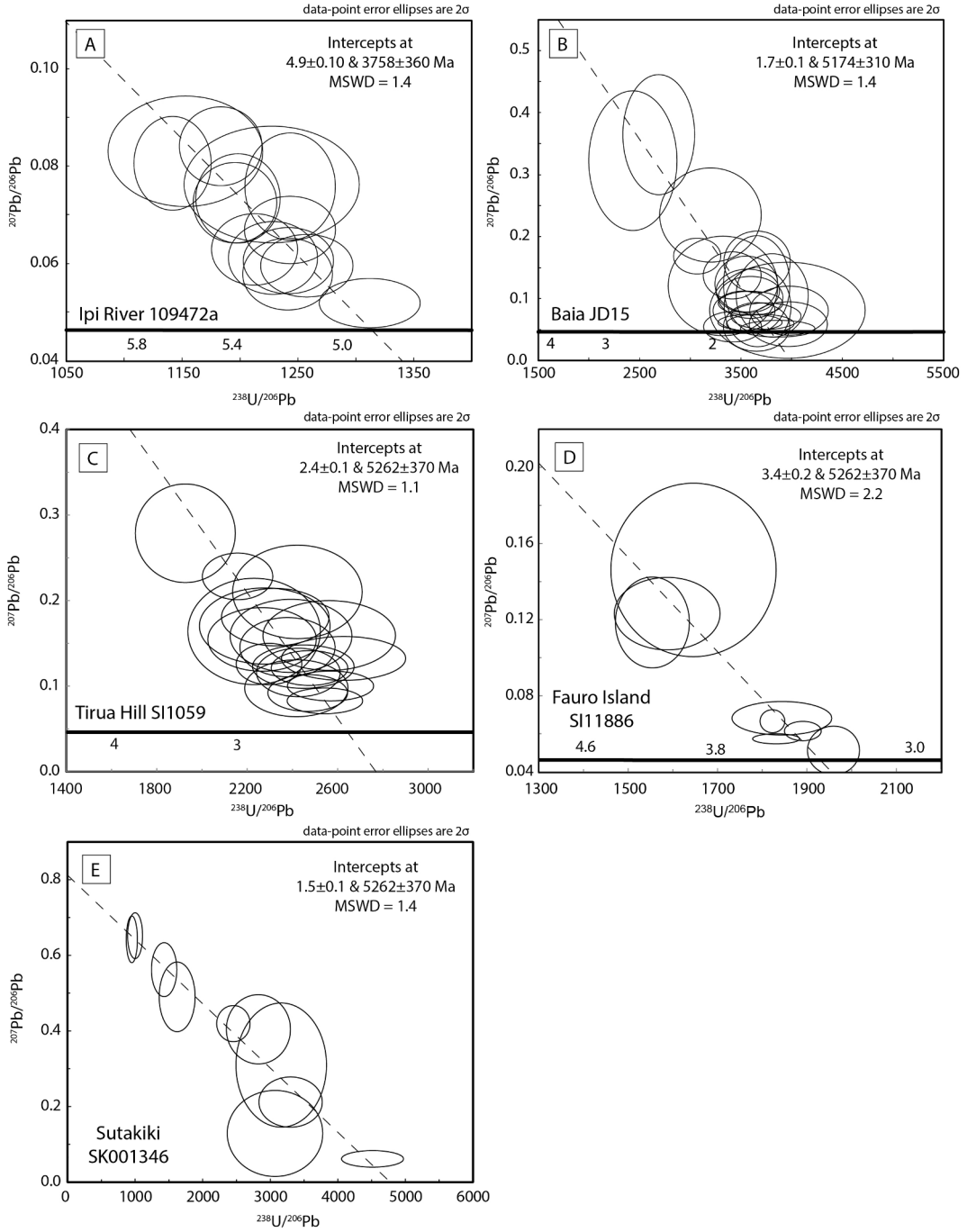

Fig. 4. U-Pb dating results for A) Ipi River 109472a; B) Baia JD15; C) Tirua Hill SI1059; D) Fauro Island SI11886; and E) Sutakiki SK001346.

location of deposit formation is according to Table 1, where these are assigned to 3-million-year time windows. In the following section, we outline the tectonic evolution of the magmatic arcs of the Papua New Guinea and Solomon Islands region, and correlate episodes of mineral deposit formation with major tectonic events, utilizing the plate tectonic reconstructions. The role of structures, both in the upper plate and as slab structures is also introduced, however, this can only be correlated for the active and recent metallogenetic systems where we have sufficient insight into the morphology and structure of the subducting plate. Such relationships between tectonics and deposit formation provided by this review of regional metallogenesis can provide a guide to the recognition of similar patterns in ancient convergent margins and serve to inform future exploration strategies.

7. Regional metallogenesis

7.1. Tectonic evolution and metallogenesis of the Melanesian arc

The Melanesian arc, comprised of New Britain, New Ireland and Bougainville of Papua New Guinea, and much of the Solomon Islands (e.g. Abbott, 1995; Kroenke, 1984; Petterson et al., 1999), represents the expression of arc magmatism related to subduction of the Pacific plate beneath the Australian plate at the Melanesian trench (Figs. 2 and 6; Petterson et al., 1999; Hall, 2002; Schellart et al., 2006; Holm et al., 2013). The early stages of subduction and arc development are poorly understood due to the paucity of known exposed Melanesian arc rocks and limited studies to date. Since the time of arc formation, however,

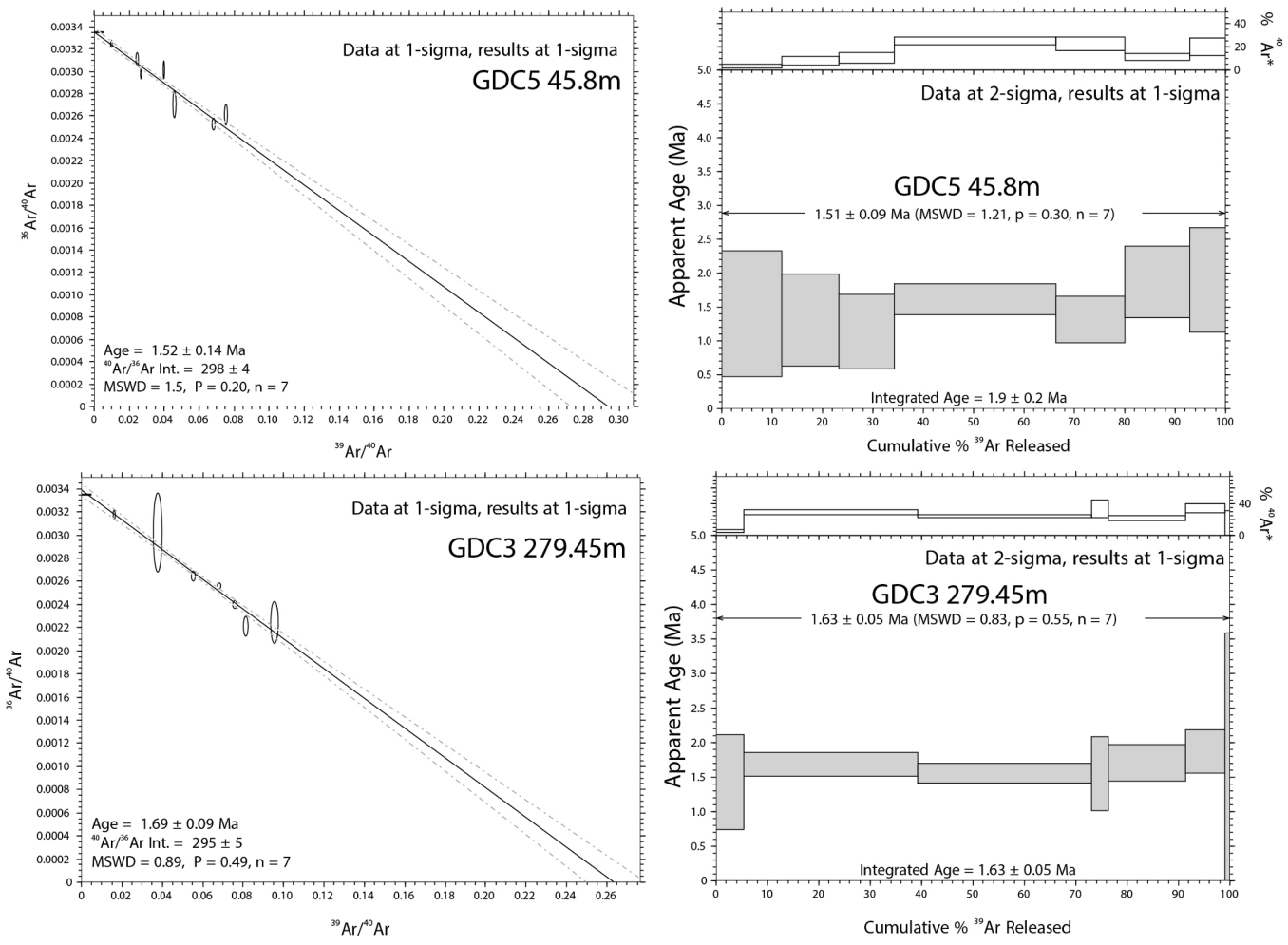

Fig. 5. Ar-Ar dating results for Gold Ridge samples GDC5 45.8 m and GDC3 279.45 m.

Melanesian arc basement has undergone complex tectonic reorganizations (Petterson et al., 1999; Hall, 2002; Schellart et al., 2006; Holm et al., 2016).

The most significant event in the history of the Melanesian arc is the collision of the 33 km thick Cretaceous Ontong Java Plateau with the Australian plate margin in the vicinity of the Solomon Islands (Kroenke, 1984; Petterson et al., 1999) at approximately 26 Ma (Fig. 6; Petterson et al., 1999; Hall, 2002; Knesel et al., 2008; Holm et al., 2013). This collision is interpreted to have caused 1) deceleration of the Australian plate motion (Knesel et al., 2008); 2) cessation of sea floor spreading in the Caroline Sea, Solomon Sea, Rennell trough and South Fiji Basin at or around 25 Ma (Davey, 1982; Hall, 2002; Gaina and Müller, 2007; Seton et al., 2016); 3) termination of magmatism in (at least) the western Melanesian arc in the earliest Miocene (Petterson et al., 1999; Lindley, 2006; Holm et al., 2013); and 4) opening of a series of intra-arc basins along the same arc from approximately the late Oligocene (Central Solomon Basin [Cowley et al., 2004; Wells, 1989]; New Hebrides intra-arc basins [Bradshaw, 1992]). Locally in New Britain, an early Miocene extensional regime is inferred from north-northeasterly extensional joint sets and associated hydrothermal activity dated at 22–23 Ma (Wilcox et al., 1973; Lindley, 2006).

Following Ontong Java collision, intense metallogenic activity occurred in the Melanesian arc. Mineral deposits are spatially distributed throughout the Melanesian arc in regions where the arc rocks of this age are outcropping (Fig. 6). The mineral deposits are distributed both adjacent to the site of Ontong Java Plateau collision (Guadalcanal and New Ireland), and distal to collision (New Britain). This suggests that mineralization was likely an arc-scale event rather than a more local process associated directly with plateau collision and stagnant or flat slab subduction (e.g. Kay and Mpodozis, 2001; Rosenbaum et al., 2005). Most deposits are porphyry Cu deposits with subsidiary epithermal deposit types; Au features mainly as a secondary commodity (Fig. 6). It is unclear whether this is a function of exhumation (e.g. erosion of high-level epithermal deposits) and currently exposed crustal levels, or whether this is influenced by the magma composition and localized fluid characteristics. The timing of formation of most Melanesian arc deposits is unfortunately poorly constrained, but based on the known interpreted deposit ages it appears that the main metallogenic episode formed shortly after the collision of the Ontong Java Plateau with the Solomon Islands (ca 24–20 Ma).

Few studies have investigated the late Oligocene-early Miocene Cu-Au mineralization within the Melanesian arc making it difficult to correlate deposit formation with specific mechanisms within the arc setting. However, post-collision mineralizing intrusions related to formation of the Simuku deposit in New Britain have been shown to hold adakite-like characteristics (e.g. high Sr/Y, HREE depletion; Holm et al., 2013). Such affinities are commonly linked to intrusion-related mineral deposits globally (e.g. Richards, 2011; Loucks, 2014). The mechanism for generating these intrusions is not yet conclusive, but Holm et al. (2013) interpreted that the intrusions must have originated from mantle-derived melt at high pressure (i.e. deep crust or mantle) or melting of a garnet-bearing source, such as eclogite or garnet amphibolite of the subducting slab or thickened arc crust (Chiaradia, 2009; Chiaradia et al., 2009; Macpherson et al., 2006; Rapp and Watson, 1995; Richards, 2011; Richards and Kerrich, 2007; Sen and Dunn, 1994).

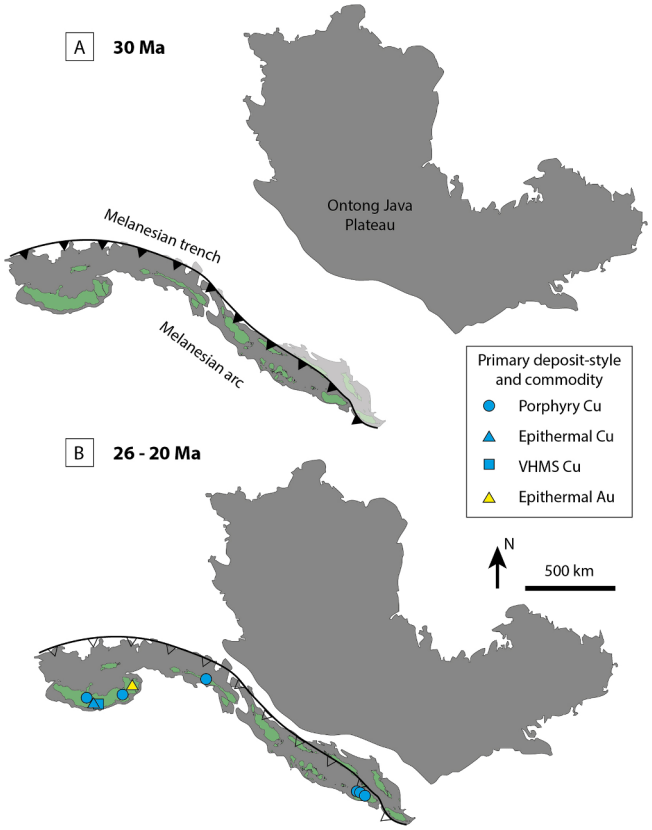

Fig. 6. Tectonic reconstruction for collision of the Ontong Java Plateau with the Melanesian arc and deposit formation for 30 Ma and 26–20 Ma. Green regions denote the present-day landmass using modern coastlines; grey regions are indicative of crustal extent using the 2000 m bathymetric contour. The reconstruction is presented here without a specific reference frame for ease of visualization, please see the reconstruction files in the supplementary material for specific reference frames. (For interpretation of the references to colour in this figure legend, the reader is referred to the web version of this article.)

7.2. Tectonic evolution and metallogenesis of the Maramuni arc

Following the arrival of the Ontong Java Plateau at the Melanesian trench, at 26 Ma (Petterson et al., 1999; Knesel et al., 2008; Holm et al., 2013), and late Oligocene arc-continent collision of the Sepik arc terranes onto the northern margin of the New Guinea Mobile Belt (Dow, 1977; Pigram and Davies, 1987; Struckmeyer et al., 1993; Abbott et al., 1994; Abbott, 1995; Crowhurst et al., 1996; Findlay, 2003), Maramuni arc magmatism intruded the New Guinea Mobile belt from the early Miocene (Dow et al., 1972; Page, 1976; Dow, 1977). As outlined above, the subduction that gave rise to the Maramuni arc is contentious, and we adopt a model of north-dipping subduction at Pocklington trough to the south of the New Guinea Mobile Belt and Papuan Peninsula (Holm et al., 2015b; a similar inference was also made by Cloos et al. (2005) and Webb et al. (2014)). However, the extent of this structure west into Indonesia is unclear. At this time (late Oligocene-early Miocene), the New Guinea Mobile Belt existed as a ribbon of marginal continental crust (e.g. Crowhurst et al., 2004) that was rifted from the Australian continent, perhaps somewhat analogous to the modern-day Lord Howe Rise and Norfolk Ridge in the Tasman Sea. There are no known significant mineral deposits formed during this first phase of arc magmatism (Fig. 7).

By ca. 12 Ma, convergence at the Pocklington trough and northward drift of the Australian continent resulted in collision with the outboard New Guinea Mobile Belt and the closure of the Pocklington Sea (Fig. 7; Cloos et al., 2005; Webb et al., 2014; Holm et al., 2015b). This event is marked by uplift in the New Guinea Orogen (Hill and Raza, 1999; Cloos et al., 2005). This change is also manifested in the magmatic record by a transition from medium-K calc-alkaline arc magmatism at ca. 12 Ma to a marked increase in crustal contribution to the magmas and less positive εHf values at ca. 9.4 Ma and 8.7 Ma, interpreted as introduction of Australian crust into the subduction zone (Holm et al., 2015b). From 12 Ma, growth of the New Guinea Orogen was driven by shortening and uplift of the New Guinea Mobile Belt and by accretion of Australian continental platform sediments that initiated the accretionary complex of the Papuan Fold and Thrust Belt (Hill and Gleadow, 1989; Hill et al., 2002; Cloos et al., 2005; Holm et al., 2015b).

Syn-orogenic magmatism of the Maramuni arc was associated with the formation of extensive 12–6 Ma mineral systems throughout mainland Papua New Guinea (Fig. 7). These deposits form a belt proximal to the site of continental collision (Lagaip and Bundi fault zones; Figs. 2 and 7), which forms the suture between the Papuan Fold and Thrust Belt and the New Guinea Mobile Belt (Dow et al., 1972; Dow, 1977; Holm et al., 2015b). The Woodlark deposit, located on the offshore extension of the Papuan Peninsula, is temporally correlative with deposits on mainland Papua New Guinea and is therefore included in this group (Figs. 1 and 7). In general, the earlier deposits associated with this metallogenic episode, which formed at ca. 12 Ma (e.g., Frieda River, Wamum and Woodlark Island), reside in the New Guinea Mobile Belt to the north of the main collisional suture, whereas the later deposits (e.g. Yandera, Kainantu and Wafi-Golpu) reside adjacent to the Lagaip and Bundi suture zones (Fig. 1). This spatial-temporal distribution is in agreement with the interpreted tectonic model of southward migrating arc magmatism (Fig. 2; Davies, 1990) in response to continental underthrusting and slab steepening (Cloos et al., 2005; Holm et al., 2015b). Mainland deposit types are typically porphyry deposits, as opposed to epithermal deposits that occur farther east on the Papuan Peninsula (Fig. 7). This may reflect variation in the level of exhumation and erosion with deeper crustal levels exposed in the New Guinea Orogen related to greater crustal shortening and uplift. In addition, there is also an observed change in the nature of mineral resources, with Cu-Au mineral systems dominating the New Guinea Orogen, whereas Au systems are more dominant farther east on the Papuan Peninsula to Woodlark Island (Fig. 7). This also correlates with a spatial change in the nature of magmatic activity, with medium-K calc-alkaline magmatism of the New Guinea Orogen transitioning to high-K calc-alkaline magmatism in southeast Papua New Guinea (e.g. Smith, 1976; Ashley and Flood, 1981; Whalen et al., 1982; Lunge, 2013; Holm et al., 2015b)

From approximately 7 Ma, uplift of the New Guinea Orogen and the apparent intensity of magmatism accelerated (Hill and Gleadow, 1989; Cloos et al., 2005). Magmatism of this age shows a clear migration to the south, forming a latest Miocene–Quaternary magmatic belt that intruded the Papuan Fold-and-Thrust Belt and the Fly Platform to the south (Fig. 2). Recent and preserved Quaternary magmatism is expressed as widespread large shoshonitic and andesitic stratovolcanoes and intrusive bodies (Page, 1976, Johnson et al., 1978), often spatially controlled by regional-scale structural lineaments (Davies, 1990; Hill et al., 2002). This magmatism is often characterized by a HREE-depleted composition indicative of melt generation or fractionation at high-pressure in the presence of garnet (Holm et al., 2015b). While investigations into the source of this magmatism has been inconclusive to date (e.g. Johnson et al., 1978; Johnson and Jaques, 1980), the most likely scenario is that post-orogenic melting was triggered by adiabatic decompression of the underlying asthenosphere in response to detachment of the stagnated Pocklington slab and collisional delamination at ca. 6 Ma (Cloos et al., 2005; Holm et al., 2015b). The current location of the detached Pocklington slab has not yet been investigated but the recognition of a high-velocity P-wave tomography anomaly beneath northern Australia (e.g. Hall and Spakman, 2002; Schellart and Spakman, 2015) may represent the detached slab.

Mineral deposits associated with the post-orogenic metallogenic episode are defined by ages of ca. 6 Ma and younger, and include

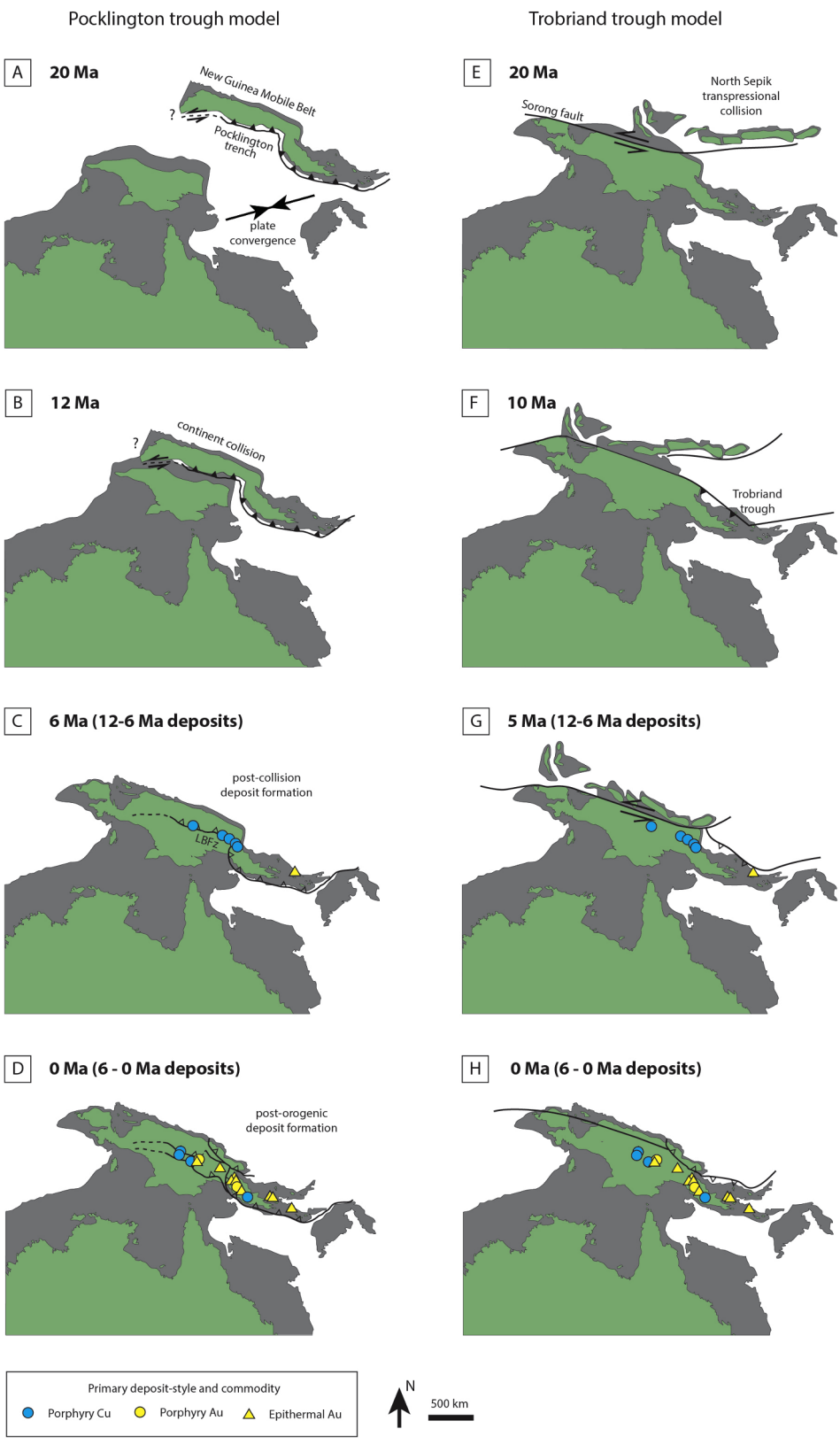

Fig. 7. Tectonic reconstruction for the period 20–0 Ma, illustrating collision of the Australian continent with the New Guinea Mobile Belt versus the Hall (2002) reconstruction model of Trobriand trough subduction. Syn-orogenic deposit formation from 12 to 6 Ma, and post-orogenic formation from 6 to 0 Ma are shown for correlation. Green regions denote the present-day landmass using modern coastlines; grey regions are indicative of crustal extent using the 2000 m bathymetric contour. The reconstruction is presented here relative to a fixed Australia reference frame for ease of visualization, please see the reconstruction files in the supplementary material for specific reference frames. (For interpretation of the references to colour in this figure legend, the reader is referred to the web version of this article.)

deposits such as Porgera, Ok Tedi and Tolukuma (Fig. 7). The spatial distribution of these deposits forms a general belt that reflects the geological setting of the earlier Maramuni arc magmatism but is more continuous along the New Guinea Orogen and Papuan Peninsula when compared to the earlier *syn*-orogenic deposits (Fig. 7). This behavior may be related to preservation. These post-orogenic deposits generally reside to the south of the 12–6 Ma deposits and are hosted within the Papuan Fold and Thrust Belt and Papuan Peninsula but there is no clear spatial trend related to the age of deposit formation internally within this group. Intrusions related to mineralization are diverse in nature, for example, intraplate alkalic basalts that host the giant Porgera gold deposit (Richards et al., 1990) are distinct within the extensive

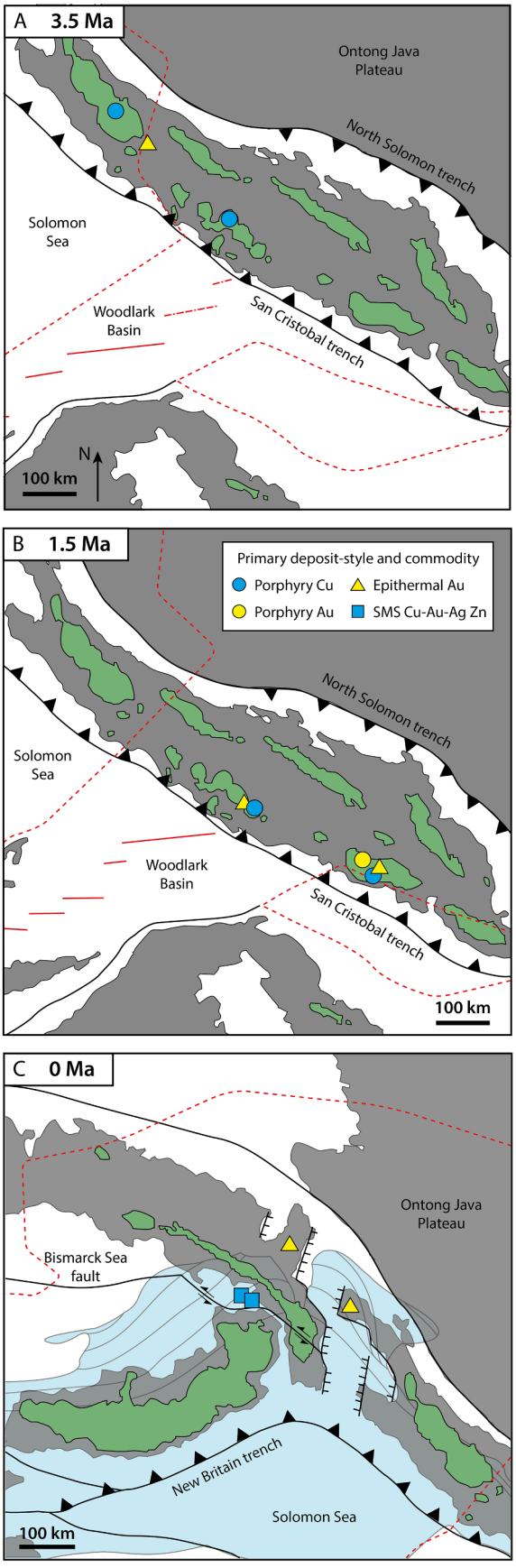

Fig. 8. Selected tectonic reconstructions and mineral deposit formation for key areas and times within the eastern Papua New Guinea and Solomon Islands region. A) Formation of the Panguna and Fauro Island Deposits above the interpreted subducted margin of the Solomon Sea plate-Woodlark Basin, and Mase deposit above the subducting Woodlark spreading center; B) Formation of the New Georgia deposits above the subducting Woodlark spreading center, and Guadalcanal deposits above the subducting margin of the Woodlark Basin; C) Formation of the Solwara deposits related to transtension along the Bismarck Sea fault above the subducting Solomon Sea plate, and deposits of the Tabar-Lihir-Tanga-Feni island arc chain related to upper plate extension (normal faulting indicated by hatched linework between New Ireland and Bougainville), while the Ladolam deposit forms above a tear in the subducting slab. Interpreted Solomon Sea slab (light blue shaded area for present-day) is from Holm and Richards (2013); the reconstructed surface extent or indicative trend of slab structure is indicated by the dashed red lines. Green regions denote the present-day landmass using modern coastlines; grey regions are indicative of crustal extent using the 2000 m bathymetric contour. The reconstruction is presented here relative to the global moving hotspot reference frame, please see the reconstruction files in the supplementary material for specific reference frames. (For interpretation of the references to colour in this figure legend, the reader is referred to the web version of this article.)

shoshonitic and high-K calc-alkaline post-orogenic magmatism (e.g. Smith, 1976, 1982; Johnson et al., 1978; van Dongen et al., 2010a; Holm and Poke, 2018). These differences highlight unexplained discrete geochemical domains within what appears to be a continuous magmatic belt. Deposits of this age are diverse and represented by porphyry and epithermal deposits with some related mineralized skarn systems. There is no clear preferred commodity type observed for the post-orogenic deposits. Gold deposits are widespread, particularly to the east (in the Papuan Peninsula). However, Cu appears to become more important in the central New Guinea Orogen with deposits such as Ok Tedi, Star Mountains and Baia (Fig. 7).

In comparison to the subduction model presented here, the alternative model invokes southwest-dipping subduction at the Trobriand trough to the north of New Guinea from the late Oligocene (Crowhurst et al., 1996; Hill and Raza, 1999; Hall, 2002). The interpretation of the Trobriand trough and associated plate margin geometry has taken various forms (Fig. 7; e.g. Davies et al., 1987; Lock et al., 1987; Hall, 2002; Schellart et al., 2006; Davies, 2012; Seton et al., 2016). Arc-continent collision at the Trobriand trough plate boundary, often in combination with the sinistral transpression across northern New Guinea (Fig. 7), is then linked to the ongoing formation of the New Guinea Orogen and associated mineral deposit formation. However, given the late Oligocene age of initial docking of the Sepik arc terranes at the northern New Guinea coast, there is a large disconnect in time (and indeed in space) between the interpreted collision event and the onset of orogenesis and mineral deposit formation from 12 Ma. Together with the recent findings from Cloos et al. (2005), Webb et al. (2014), and Holm et al. (2015b), this supports the use of the Pocklington trough subduction model over that of the Trobriand trough.

7.3. Tectonic evolution and metallogenesis of the New Britain and Solomon arcs

Following collision of the Australian continent with Papua New Guinea and cessation of subduction at the Pocklington trough (Cloos et al., 2005; Holm et al., 2015b) by ca. 10 Ma, the regional tectonics had undergone reorganization and convergence was established at the New Britain and San Cristobal trenches (e.g. Petterson et al., 1999). This period of tectonic reorganization is characterized by the ongoing development of regional microplate tectonics, marked by rapid changes in the plate kinematics of discrete terranes and the localized, simultaneous development of extensional and contractional tectonics.

Retreat of the western New Britain trench from ca. 6 Ma led to back-arc extension and rifting that initiated formation of the Bismarck Sea (Taylor, 1979; Holm et al., 2016). Anticlockwise rotation of the Solomon Sea, linked to hinge retreat at the western New Britain trench (Wallace et al., 2014; Ott and Mann, 2015; Holm et al., 2016), resulted in decoupling of the Solomon Sea plate from the Australian plate, which initiated minor underthrusting of the Solomon Sea plate at the Trobriand trough (Holm et al., 2016), and rotational extension and rifting in the Woodlark Basin from ca. 6 Ma (Taylor et al., 1999; Wallace et al., 2014; Holm et al., 2016). This period of tectonic reorganization from ca. 10 to 6 Ma reflects an overall setting dominated by extensional tectonics that does not seem to be linked to known mineral deposits.

Subduction of the active Woodlark spreading center at the San Cristobal trench from ca. 5 Ma had important implications for the geological evolution of the Solomon Islands (Chadwick et al., 2009; Holm et al., 2016). The timing for initial ridge subduction overlaps with the onset of crustal shortening across the Solomon Islands and convergence at the North Solomon trench adjacent to the Ontong Java Plateau (Petterson et al., 1997, 1999; Cowley et al., 2004; Mann and Taira, 2004; Phinney et al., 2004; Taira et al., 2004; Holm et al., 2016). Subduction of the spreading center adjacent to the central Solomon Islands also caused extensive arc magmatism, which included high-Mg andesites and adakite-like geochemical signatures (Mann et al., 1998; Chadwick et al., 2009; Schuth et al., 2009). This was exemplified by formation of the New Georgia group of islands that coincide with the location of spreading ridge subduction (Fig. 8; Petterson et al., 1999; Chadwick et al., 2009; Schuth et al., 2009; Holm et al., 2016), and host the Tirua, Mase and Kele River deposits (Figs. 1 and 8a). Reconstructions show that the New Georgia islands and associated ore deposits have been located adjacent to the subducting spreading center since at least the middle Pliocene (Fig. 8a). The first absolute geochronological constraints from this area (Tirua Hill; Fig. 4) indicate that mineralization occurred around 2.4 Ma. Cross-cutting relationships with island arc picrites, which signify the effects of spreading ridge subduction on the arc magmatism, indicate that mineralization must post-date initial spreading ridge subduction. The slab window generated by spreading ridge subduction is potentially the cause of one of few currently active volcanic centers in the Solomon arc and a potentially mineralizing hydrothermal system at Savo Island (Smith et al., 2009, Smith et al., 2010, Smith et al., 2011). This suggests a prolonged (~2.5 Myr) influence of direct ridge subduction on magmatism and the formation of mineral deposits.

In addition to spreading center subduction, a correlation also exists for the location and timing of deposit formation with subduction of the Woodlark Basin marginal structures. Mineralization on Guadalcanal, at the southeast margin of the Woodlark Basin, occurred at ca. 1.6 Ma, approximately contemporaneously with the emplacement of the Koloula Porphyry Complex (1.6–1.45 Ma; Tapster et al., 2016), Sutakiki epithermal-porphyry prospect (1.5 Ma) and Gold Ridge low sulfidation epithermal deposit (1.6–1.5 Ma; Fig. 8b) along an arc-normal (NNE-SSW) transpressive structural corridor in central Guadalcanal (Hackman, 1980; Swiridiuk, 1998; Tapster et al., 2011, 2016). Given the nature of described fault-intrusion relationships at Koloula, the arc-normal deformation that controlled mineralization along the corridor was only active shortly before 1.6 Ma and had terminated by ca. 1.5 Ma (Tapster et al., 2016). The close temporal association of porphyry to epithermal deposits (~100 kyrs) along a spatial corridor that extends over 30 km preclude a direct genetic link between deposits and highlight the critical role that short-lived upper plate structures can have on controlling mineralization. The central NNE-SSW corridor in Guadalcanal runs parallel to a similar set of lineaments in the west of the island, currently under a much thicker Pliocene-Pleistocene volcanic cover. The orientation of structures across the island and their coincidence with the subduction of the southeast margin of the Woodlark Basin (Fig. 8b) suggests that there may be a relationship between the upper-plate structure and subducting topographic high (Tapster et al., 2011). Subduction of the young, hot and buoyant Woodlark Basin crust potentially acted as an indentor, generating structural controls for magma emplacement and mineralization. A similar relationship exists for the location of subduction of the northwest margin of the Woodlark Basin and formation of the Panguna and Fauro Island deposits in the adjacent overriding plate at ca. 3.5–3.4 Ma (Fig. 8a).

Farther west, the Tabar-Lihir-Tanga-Feni island arc chain of eastern Papua New Guinea hosts the Ladolam, Simberi and Kabang deposits. In this area, differential plate motion between the Solomon Islands and the North Bismarck microplate resulted in intra-arc extension between the islands of New Ireland and Bougainville (Holm et al., 2016). An extensional origin for the Tabar-Lihir-Tanga-Feni island arc chain is supported by geochemical studies, which suggested that the volatile-rich, silica-undersaturated, high-K calc-alkaline basaltic lavas were produced by adiabatic decompression melting of subduction-modified upper mantle (Patterson et al., 1997; Stracke and Hegner, 1998). This region therefore represents an upper plate extensional setting, contemporaneously with tearing of the subducting Solomon Sea slab (Fig. 8c; Holm et al., 2013). The reasons for development of the slab tear are not understood, but tears in the subducting slab such as this are interpreted to promote increased fluid flux and metal transport within the mantle, resulting from a larger exposure of the subducting slab to the surrounding asthenospheric mantle (Richards and Holm, 2013). From this setting it cannot be conclusively determined which of the two settings, upper plate extension, or tearing of the subducted slab, contribute more to potential formation of mineral deposits. However, correlation in the location of the Ladolam deposit above the interpreted slab tear at the time of formation suggests that it was a combination of the two factors that likely contributed to mineralization.

In the Bismarck Sea, the Solwara deposits of the eastern Bismarck Sea region lie along the Bismarck Sea fault, a transtensional structure that accommodated sinistral motion between the North and South Bismarck microplates as well as opening of the Manus Basin (Figs. 1 and 8c; Taylor, 1979; Martinez and Taylor, 1996; Holm et al., 2016). This setting is similar to that of the Tabar-Lihir-Tanga-Feni island arc chain outlined above, where occurrence of a dilational upper plate structure likely acted as a preferential conduit that promoted subduction-related magma flux (Fig. 8c). This example emphasizes the important role of upper plate extension in localizing deposit formation. Preservation is also a major factor for the Solwara seafloor massive sulfide deposit, where the high-grade, small tonnage nature of the deposit type is susceptible to erosion or burial beneath younger sediments.

8. Discussion

Mineral deposit exploration methodology is currently undergoing new developments driven by large databases and advances in technological capabilities (e.g. Cawood and Hawkesworth, 2015; Butterworth et al., 2016). Such models provide a useful regional context for deposit formation and an understanding of the large-scale conditions under which deposits are likely to form. However, at a smaller scale there are always exceptions to these conditions that arise from dynamic geological settings. For example, in the southwest Pacific and Southeast Asia episodes of continental accretion took place throughout the Cenozoic (Audley-Charles, 1981; Petterson et al., 1999; Hill and Hall, 2003; Holm et al., 2013; Holm et al., 2015b), and microplate tectonics has been active at ever smaller scales (Wallace et al., 2004; Holm et al., 2016). Through combining our knowledge of plate boundary-scale processes with inherent regional- and district-scale aberrations in these Earth systems we can advance our understanding of metallogenesis and achieve greater success in mineral exploration.

Comparison of the location, timing, metal content and the frequency of mineral deposit formation/occurrence with episodes of tectonic reorganization (Fig. 9) reveals a strong correlation. Melanesian arc metallogenesis (ca. 24–20 Ma), related to collision of the Ontong Java Plateau and cessation of subduction at the Melanesian trench, was a Cu-

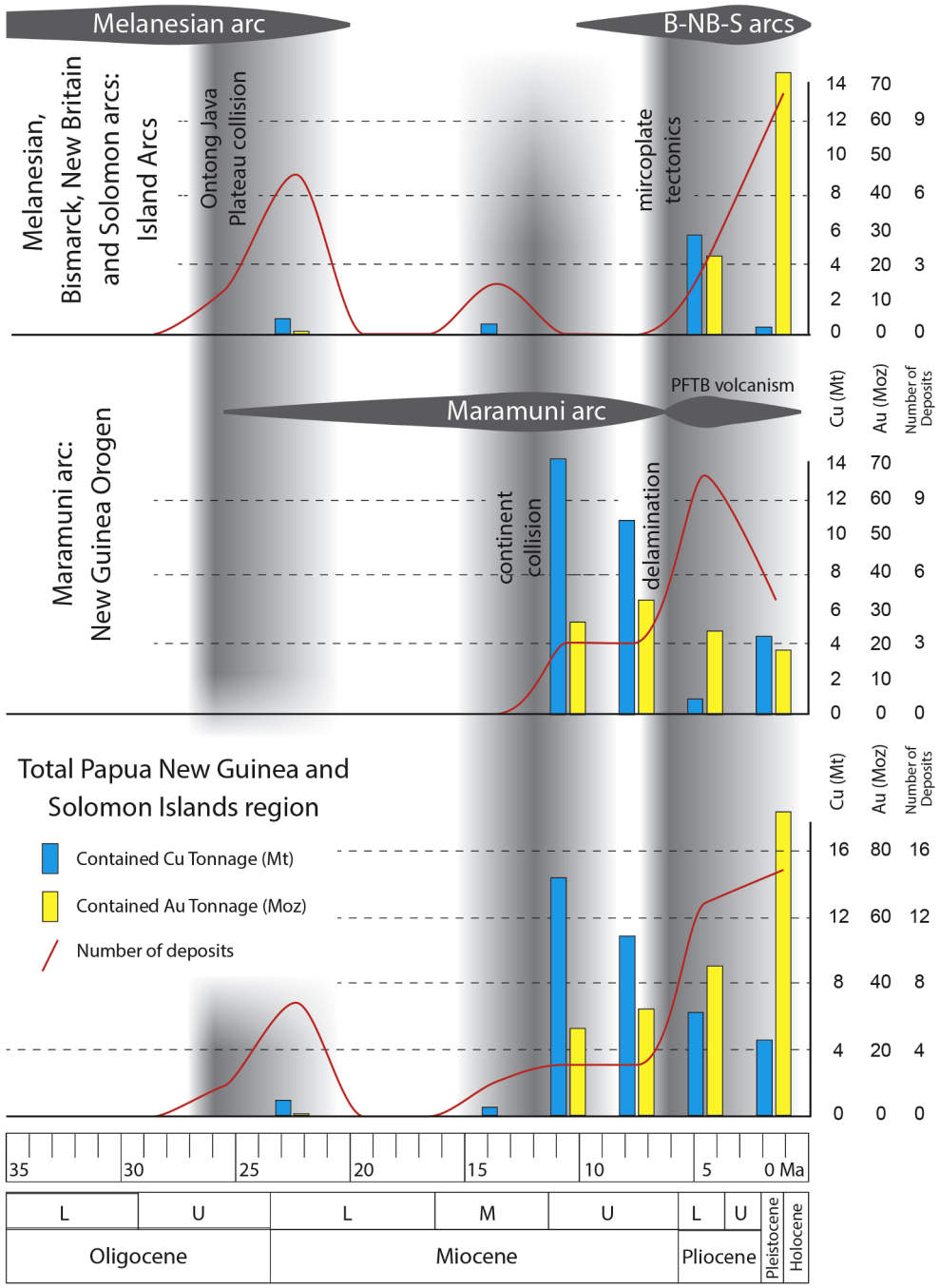

Fig. 9. Mineral endowment for Papua New Guinea and Solomon Islands through time. Total contained Cu and Au tonnage are shown at time of deposit formation, with number of deposits in 3 Myr bins. Deposits are differentiated into the island arc terranes for the Melanesian, West Bismarck, New Britain and Solomon arcs, and the New Guinea Orogen with deposits related to the Maramuni arc.

rich but relatively minor event in terms of total known metal endowment. In contrast, the overprinting West Bismarck, New Britain and Solomon arcs host Cu-Au mineral deposits that formed during a distinct metallogenic episode from ca. 6 Ma and became decisively Au-rich from ca. 3 Ma (Fig. 9). This may represent a major episode of intrusive activity and metal-endowment within the region, which was linked to the onset of regional microplate tectonics from ca. 6 Ma. Correlation of the New Guinea Orogen metallogenesis with regional tectonics reveals two discrete episodes of deposit formation related to different tectonic events. The first deposit-forming event related to Australian continental collision, waning medium-K calc-alkaline Maramuni arc magmatism and orogenesis from ca. 12 Ma up to 6 Ma has a large copper-rich mineral endowment but few known deposits (Fig. 9). The later deposit-forming event from ca. 6 Ma may have occurred in response to crustal delamination. It is characterized by a large number of known deposits related to high-K calc-alkaline to shoshonitic (and minor intra-plate alkalic) magmatism, but these represent a smaller endowment in comparison to the 12–6 Ma event, with no clear preference in commodity. There is no correlation between the composition of the magmatism and occurrences of mineralization with a broad compositional spectrum from medium-K calc-alkaline through to shoshonitic intrusives and even intra-plate alkalic compositions related to deposits in the New Guinea Orogen and Papuan Peninsula; adakitic compositions, however, are commonly linked to mineral deposits throughout the islands of eastern Papua New Guinea and the Solomon Islands. Importantly, formation of deposits does occur over narrow time intervals

that suggest association with regional and discrete tectonic events, such as those interpreted to occur in association with subduction at the Pocklington trough.

An evaluation of the nature and variability of the diverse geodynamic settings for deposit emplacement through time, and the relationship with the southwest Pacific magmatic arcs and associated subduction dynamics, can provide crucial insights into the array of deposit settings at ancient convergent margins. For example, given current plate motion and convergence rates, it is expected that the Ontong Java Plateau will collide with the Australian continent in approximately 20 million years, resulting in a vast orogen along northeast Australia. The orogen will comprise accreted and highly strained terranes that include the island arcs of eastern Papua New Guinea and the Solomon Islands, and the already composite terranes of mainland Papua New Guinea. In this orogen, the different episodes of mineral deposit formation described above will likely be superimposed on one another. This underscores the importance of recognizing different terranes and tectonic complications in present-day convergent margins, such as the southwest Pacific, to successfully unravel ancient collisional margins such as the North American Cordillera (e.g. Sillitoe, 2008) or the Tasmanides of eastern Australia (e.g. Cooke et al., 2007; Glen et al., 2007). This study provides a benchmark for our understanding of the tectonic evolution and metallogenesis of Papua New Guinea and the Solomon Islands, and an analogue with which to compare complex convergent margins globally. By developing such an understanding of the intricacies and aberrations that exist within convergent margin tectonics we can further develop and refine regional exploration models.

9. Conclusions

A strong correlation between deposit formation and episodes of tectonic reorganization is interpreted for the Papua New Guinea and the Solomon Islands region. The first metallogenic event is result of collision of the Ontong Java Plateau with the Solomon Islands at ca. 26 Ma and correlates with formation of copper-rich mineral deposits throughout the Melanesian arc between ca. 24 and 20 Ma. Subsequent collision of the Australian continent with Papua New Guinea at ca. 12 Ma resulted in two discernible metallogenic events: 1) formation of ca. 12–6 Ma copper-rich mineral deposits associated with medium-K to high-K calc-alkaline magamtism and development of the New Guinea Orogen, and 2) formation of ca. 6–0 Ma gold and copper mineral deposits related to delamination of the stagnated slab following collision, and genetically linked to diverse high-K calc-alkaline and alkaline magmatic compositions. The emergence of microplate tectonics in eastern Papua New Guinea and the Solomon Islands from ca. 6 Ma resulted in highly dynamic and discrete kinematic settings throughout the region. Prospective settings for gold-rich deposit formation are interpreted to be related to the localization of mineralized corridors above tearing of a subducted slab and development of slab windows, or upper plate structures related to extension or shortening that promote magma-flux from the underlying mantle and act as an upper plate conduit for fluid-flow (e.g., eastern Bismarck Sea Fault). These findings suggest that a good understanding of geodynamic settings through time, both on the scale of regional subduction zones and district-scale structure, have the potential to contribute to prospectivity studies and the generation of new exploration targets at regional scales.

Acknowledgments

R. Holm thanks Simon Richards, Carl Spandler and Yi Hu for fruitful discussions and analytical assistance, and also J. Espi, Petromin PNG and Barrick Australia for support. S. Tapster acknowledges the funding from, and thanks the British Geological Survey University Funding Initiative PhD studentship (S176), NIGFSC (IP-1212-1110), and SEG Newmont Student Research grant (2274). This work could not have been possible without support provided by the Solomon Island Geological Survey and Ministry of Mines, Newmont Mining, SolGold (A.R.M) and the team of Allied Gold. Nick Roberts and Vanessa Pashley of NIGL are thanked for their analytical assistance. Robert Hall, Peter Holling, Georges Beaudoin and an anonymous reviewer are thanked for their comments and feedback on previous versions of this manuscript; anonymous reviewers and Franco Pirajno are also thanked for constructive reviews and editorial assistance on the manuscript.

Appendix A. Supplementary data

Supplementary data to this article can be found online at https://doi.org/10.1016/j.oregeorev.2018.11.007.

References

Abbott, L.D., 1995. Neogene tectonic reconstruction of the Adelbert-Finisterre-New Britain collision, northern Papua New Guinea. J. SE Asian Earth Sci. 11, 33–51.
Abbott, L.D., Silver, E.A., Galewsky, J., 1994. Structural evolution of a modern arc–continent collision in Papua New Guinea. Tectonics 13, 1007–1034.
Adshead, N.D., 1997. The setting and characteristics of the Umuna epithermal gold-silver deposit, Misima Island, Papua New Guinea. In: Hancock, G., 1997. Proceedings of the Geology, Exploration and Mining Conference, Madang. Australasian Institute of Mining and Metallurgy, Parkville, 1–7.
Arnold, G.O., Griffin, T.J., 1978. Intrusions and porphyry copper prospects of the Star Mountains, Papua New Guinea. In: Gustafson, L.B., Titley, S.R. (Eds.), Porphyry copper deposits of the southwestern Pacific islands and Australia. Economic Geology, pp. 785–795.
Ashley, P.M., Flood, R.H., 1981. Low-K tholeiites and high-K igneous rocks from Woodlark Island, Papua New Guinea. J. Geol. Soc. Aust. 28, 227–240.
Audley-Charles, M.G., 1981. Geometrical problems and implications of large scale overthrusting in the Banda Arc–Australian margin collision zone. In: McClay, K.R. (Ed.), Thrust and Nappe Tectonics: Geological Society of London Special Publication 9, 407–416.
Baldwin, S.L., Fitzgerald, P.G., Webb, L.E., 2012. Tectonics of the New Guinea Region. Annu. Rev. Earth Planet. Sci. 40, 495–520.
Benes, V., Scott, S.D., Binns, R.A., 1994. Tectonics of rift propagation into a continental margin: western Woodlark Basin, Papua New Guinea. J. Geophys. Res. 99, 4439–4455.
Boyden, J.A., Müller, R.D., Gurnis, M., Torsvik, T.H., Clark, J.A., Turner, M., Ivey-Law, H., Watson, R.J., Cannon, J.S., 2011. Next-generation plate-tectonic reconstructions using GPlates. In: Keller, G.R., Baru, C. (Eds.), Geoinformatics: Cyberinfrastructure for the Solid Earth Sciences. Cambridge University Press, pp. 95–114.
Bradshaw, M., 1992. South West Pacific Data Package, BMR-APIRA Phanerozoic History of Australia Project. Record 1992/41, Palaeogeography 43. Bureau of Mineral Resources, Geology and Geophysics, and the Petroleum Division of the Australian Mineral Industry Research Association.
Burkett, D., Graham, I., Spencer, L., Lennox, P., Cohen, D., Zwingmann, H., Lau, F., Kelly, B., Cendon, D., 2015. The Kulumadau epithermal breccia-hosted gold deposit, Woodlark Island, Papua New Guinea. Proceeding PACRIM Congress, Hong Kong, China.
Butterworth, N., Steinberg, D., Müller, R.D., Williams, S., Merdith, A.S., Hardy, S., 2016. Tectonic environments of South American porphyry copper magmatism through time revealed by spatiotemporal data mining. Tectonics 35, 2847–2862.
Carswell, J.T., 1990. Wau gold deposits. Australasian Inst. Min. Metall. Monogr. Ser. 14, 1763–1767.
Cawood, P.A., Hawkesworth, C.J., 2015. Temporal relations between mineral deposits and global tectonic cycles. In: Jenkin, G.R.T., Lusty, P.A.J., McDonald, I., Smith, M.P., Boyce, A.J., Wilkinson, J.J. (Eds.), Ore Deposits in an Evolving Earth. Geological Society. Special Publications, London, pp. 9–21.
Chadwick, J., Perfit, M., McInnes, B., Kamenov, G., Plank, T., Jonasson, I., Chadwick, C., 2009. Arc lavas on both sides of a trench: Slab window effects at the Solomon Islands triple junction, SW Pacific. Earth Planet. Sci. Lett. 279, 293–302.
Chapple, K.G., Ibil, S., 1998. Gameta gold deposit. Australasian Inst. Min. Metall. Monogr. Ser. 22, 849–854.
Chiaradia, M., 2009. Adakite-like magmas from fractional crystallization and melting-assimilation of mafic lower crust (Eocene Macuchi arc, Western Cordillera, Ecuador). Chem. Geol. 265, 468–487.
Chiaradia, M., Müntener, O., Beate, B., Fontignie, D., 2009. Adakite-like volcanism of Ecuador: lower crust magmatic evolution and recycling. Contrib. Miner. Petrol. 158, 563–588.
Chivas, A.R., McDougall, I., 1978. Geochronology of Koloula-Porphyry-Copper-Prospect, Guadalcanal, Solomon-Islands. Econ. Geol. 73, 678–689.
Cloos, M., Sapiie, B., van Ufford, A.Q., Weiland, R.J., Warren, P.Q., McMahon, T.P., 2005. Collisional delamination in New Guinea: the geotectonics of subducting slab breakoff. Geol. Soc. Am., Spec. Pap. 400.
Cooke, D.R., Hollings, P., Walshe, J.L., 2005. Giant porphyry deposits: characteristics, distribution, and tectonic controls. Econ. Geol. 100, 801–818.
Cooke, R.A., Wilson, A.J., House, M.J., Wolfe, R.C., Walshe, J.L., Lickford, V., Crawford, A.J., 2007. Alkalic porphyry Au-Cu and associated mineral deposits of the Ordovician to Early Silurian Macquarie Arc, New South Wales. Aust. J. Earth Sci. 54, 445–463.
Cooper, P., Taylor, B., 1987. Seismotectonics of New Guinea: a model for arc reversal

following arc-continent collision. Tectonics 6, 53–67.
Corbett, G.J., Leach, T.M., 1998. Southwest Pacific Rim Gold-Copper Systems: Structure, Alteration, and Mineralization. Society of Economic Geologists, pp. 234.
Cowley, S., Mann, P., Coffin, M.F., Shipley, T.H., 2004. Oligocene to Recent tectonic history of the Central Solomon intra-arc basin as determined from marine seismic reflection data and compilation of onland geology. Tectonophysics 389, 267–307.
Craig, M.S., Warvakai, K., 2009. Structure of an active foreland fold and thrust belt, Papua New Guinea. Aust. J. Earth Sci. 56, 719–738.
Crowhurst, P.V., Hill, K.C., Foster, D.A., Bennett, A.P., 1996. Thermochronological and geochemical constraints on the tectonic evolution of northern Papua New Guinea. Geol. Soc., London, Special Publications 106, 525–537.
Crowhurst, P.V., Maas, R., Hill, K.C., Foster, D.A., Fanning, C.M., 2004. Isotopic constraints on crustal architecture and Permo-Triassic tectonics in New Guinea: possible links with eastern Australia. Aust. J. Earth Sci. 51, 107–122.
Davey, F.J., 1982. The structure of the South Fiji Basin. Tectonophysics 87, 185–241.
Davies, H.L., 1990. Structure and evolution of the border region of New Guinea. In: Carman, G.J., Carman, Z. (Eds.), Petroleum exploration in Papua New Guinea. Proceedings of the First PNG Petroleum Convention. PNG Chamber of Mines and Petroleum, Port Moresby, pp. 245–269.
Davies, H.L., 2012. The geology of New Guinea – the cordilleran margin of the Australian continent. Episodes 35, 87–102.
Davies, H.L., Lock, J., Tiffin, D.L., Honza, E., Okuda, Y., Murakami, F., Kisimoto, K., 1987. Convergent tectonics in the Huon Peninsula region, Papua New Guinea. Geo-Mar. Lett. 7, 143–152.
DeMets, C., Gordon, R.G., Argus, D.F., 2010. Geologically current plate motions. Geophys. J. Int. 181, 1–80.
Denham, D., 1969. Distribution of Earthquakes in the New Guinea-Solomon Islands region. J. Geophys. Res. 74, 4290–4299.
Dow, D.B., 1977. A geological synthesis of Papua New Guinea. Bureau of Mineral Resources. Geol. Geophys. 201, 41.
Dow, D.B., Smit, J.A.J., Bain, J.H.C., Ryburn, R.J., 1972. Geology of the South Sepik Region, New Guinea. Bureau of Mineral Resources, Geology and. Geophysics 133, 87.
Dugmore, M.A., Leaman, P.W., 1998. Mount Bini copper-gold deposit. Australasian Inst. Min. Metall. Monogr. Ser. 22, 843–848.
Dunkley, P.N., 1986. Geology of the New Georgia Group, Solomon Islands. British Geological Survey Overseas Directorate, British Technical Cooperation Project, Western Solomon Islands Geological Mapping Project (21).
Findlay, R.H., 2003. Collision tectonics of northern Papua New Guinea: key field relationships demand a new model. In: Hillis, R.R., Müller, R.D. (Eds.), Evolution and Dynamics of the Australian Plate. Geological Society of Australia Special Publication 22 and Geological Society of America Special Paper 372, 291–308.
Gaina, C., Müller, D., 2007. Cenozoic tectonic and depth/age evolution of the Indonesian gateway and associated back-arc basins. Earth Sci. Rev. 83, 177–203.
Garwin, S., Hall, R., Watanabe, Y., 2005. Tectonic setting, geology, and gold and copper mineralization in Cenozoic magmatic arcs of Southeast Asia and the west Pacific. Economic Geology 100th Anniversary Volume 891–930.
Glen, R.A., Crawford, A.J., Cooke, D.R., 2007. Tectonic setting of porphyry Cu-Au mineralization in the Ordovician-Early Silurian Macquarie Arc, Eastern Lachlan Orogen, New South Wales. Aust. J. Earth Sci. 54, 465–479.
Gow, P.A., Walshe, J.L., 2005. The role of preexisting geologic architecture in the formation of giant porphyry-related Cu ± Au deposits: Examples from New Guinea and Chile. Econ. Geol. 100, 819–833.
Hackman, B.D., 1980. The geology of Guadalcanal, Solomon Islands. Overseas memoirs HM Stationery Office, 6, 1−115.
Hall, R., 2002. Cenozoic geological and plate tectonic evolution of SE Asia and the SW Pacific: computer-based reconstructions, model and animations. J. Asian Earth Sci. 20, 353–431.
Hall, R., Spakman, W., 2002. Subducted slabs beneath the eastern Indonesia-Tonga region: insights from tomography. Earth Planet. Sci. Lett. 201, 321–336.
Hall, R.J., Britten, R.M., Henry, D.D., 1990. Frieda River copper-gold deposits. Australas. Institue Min. Metall. Minigraph Ser. 14, 1709–1715.
Hill, K.C., Gleadow, A.J.W., 1989. Uplift and thermal history of the Papuan Fold Belt, Papua New Guinea: apatite fission track analysis. Aust. J. Earth Sci. 36, 515–539.
Hill, K.C., Hall, R., 2003. Mesozoic-Cenozoic evolution of Australia's New Guinea margin in a west Pacific context. In: Hillis R.R., Müller, R.D. (Eds.) Evolution and Dynamics of the Australian Plate: Geological Society of Australia Special Publication 22, and Geological Society of America Special Paper, 372, 265–290.
Hill, K.C., Kendrick, R.D., Crowhurst, P.V., Gow, P.A., 2002. Copper-gold mineralisation in New Guinea: tectonics, lineaments, thermochronology and structure. Aust. J. Earth Sci. 49, 737–752.
Hill, K.C., Raza, A., 1999. Arc–continent collision in Papua Guinea: Constraints from fission track thermochronology. Tectonics 18, 950–966.
Hine, R., Bye, S.M., Cook, F.W., Leckie, J.F., Torr, G.L., 1978. The Esis porphyry copper deposit, East New Britain, Papua New Guinea. Econ. Geol. 73, 761–767.
Holm, R.J., Poke, B., 2018. Petrology and crustal inheritance of the Cloudy Bay Volcanics as derived from a fluvial conglomerate, Papuan Peninsula (Papua New Guinea): An example of geological inquiry in the absence of in situ outcrop. Cogent Geosci. 4, 1450198.
Holm, R.J., Richards, S.W., 2013. A re-evaluation of arc-continent collision and along-arc variation in the Bismarck Sea region, Papua New Guinea. Aust. J. Earth Sci. 60, 605–619.
Holm, R.J., Rosenbaum, G., Richards, S.W., 2016. Post 8 Ma reconstruction of Papua New Guinea and Solomon Islands: Microplate tectonics in a convergent plate boundary setting. Earth Sci. Rev. 156, 66–81.
Holm, R.J., Spandler, C., Richards, S.W., 2013. Melanesian arc far-field response to collision of the Ontong Java Plateau: Geochronology and pertrogenesis of the Simuku Igneous Complex, New Britain, Papua New Guinea. Tectonophysics 603, 189–212.
Holm, R.J., Richards, S.W., Rosenbaum, G., Spandler, C., 2015a. Disparate Tectonic Settings for Mineralisation in an Active Arc, Eastern Papua New Guinea and the Solomon Islands. Proceedings of PACRIM 2015 Congress, Hong Kong, China.
Holm, R.J., Spandler, C., Richards, S.W., 2015b. Continental collision, orogenesis and arc magmatism of the Miocene Maramuni arc, Papua New Guinea. Gondwana Res. 28, 1117–1136.
Hutchison, D.S., Norvick, M.S., 1980. Geology of the North Sepik Region, Papua New Guinea. Bureau of Mineral Resources. Geol. Geophys. 1980/24 67.
Hutton, M.J., Akiro, A.K., Cannard, C.J., Syka, M.C., 1990. Kerimenge gold prospect. Australas. Inst. Min. Metall. Monogr. Ser. 24, 1769–1772.
Johnson, R.W., Jaques, A.L., 1980. Continent-arc collision and reversal of arc polarity: New interpretations from a critical area. Tectonophysics 63, 111–124.
Johnson, R.W., Mackenzie, D.E., Smith, I.E.M., 1978. Delayed partial melting of subduction-modified mantle in Papua New Guinea. Tectonophysics 46, 197–216.
Kay, S.M., Mpodozis, C., 2001. Central Andean ore deposits linked to evolving shallow subduction systems and thickening crust. GSA Today 11, 4–9.
Knesel, K.M., Cohen, B.E., Vasconcelos, P.M., Thiede, D.S., 2008. Rapid change in drift of the Australian plate records collision with Ontong Java plateau. Nature 454, 754–757.
Kroenke, L.W., 1984. Cenozoic tectonic development of the southwest Pacific. U.N. ESCAP, CCOP/SOPAC Tech. Bull. 6.
Langmead, R.P., McLeod, R.L., 1990. Tolukuma gold deposit. Australas. Inst. Min. Metall. 14, 1777–1781.
Lindley, I.D., 2006. Extensional and vertical tectonics in the New Guinea islands: implications for island arc evolution. Supplement to Scalera, G., Lavecchia, G., Frontiers in sciences: new ideas and interpretation. Ann. Geophys. 49 (1).
Lindley, I.D., 1990. Wild Dog gold deposit. Australasian Inst. Min. Metall. Monogr. Ser. 14, 1789–1792.
Lock, J., Davies, H.L., Tiffin, D.L., Murakami, F., Kisimoto, K., 1987. The Trobriand subduction system in the western Solomon Sea. Geo-Mar. Lett. 7, 129–134.
Loucks, R.R., 2014. Distinctive composition of copper-ore-forming arc magmas. Aust. J. Earth Sci. 61, 5–16.
Lunge, M., 2013. A mineralogical, geochemical and geochronological study of the Golpu and Nambonga North porphyry copper-gold systems, Wafi-Golpu Mineral District, Papua New Guinea. Unpublished MSc thesis. University of Papua, New Guinea, pp. 156p.
Macpherson, C.G., Dreher, S.T., Thirlwall, M.F., 2006. Adakites without slab melting: High pressure differentiation of island arc magma, Mindanao, the Philippines. Earth Planet. Sci. Lett. 243, 581–593.
Mann, P., Taira, A., 2004. Global tectonic significance of the Solomon Islands and Ontong Java Plateau convergent zone. Tectonophysics 389, 137–190.
Mann, P., Taylor, F.W., Lagoe, M.B., Quarles, A., Burr, G., 1998. Accelerating late Quaternary uplift of the New Georgia Island Group (Solomon island arc) in response to subduction of the recently active Woodlark spreading center and Coleman seamount. Tectonophysics 295, 259–306.
Martinez, F., Taylor, B., 1996. Backarc spreading, rifting, and microplate rotation, between transform faults in the Manus Basin. Mar. Geophys. Res. 18, 203–224.
McInnes, B.I.A., 1992. A glimpse of ephemeral subduction zone processes from Simberi Island, Papua New Guinea. University of Ottawa.
McNeil, P.A., 1990. Wapolu gold deposit, Fegusson Island. Australas. Inst. Min. Metall. Monogr. Ser. 14, 1783–1788.
Moyle, A.J., Doyle, B.J., Hoogvliet, H., Ware, A.R., 1990. Ladolam Gold Deposit, Lihir Island. In: Geology of the mineral deposits of Australia and Papua New Guinea. The Australasian Institute of Mining and Metallurgy, Melbourne, pp. 1793–1805.
Müller, R.D., Seton, M., Zahirovic, S., Williams, S.E., Matthews, K.J., Wright, N.W., Shephard, G.E., Maloney, K.T., Barnett-Moore, N., Hosseinpour, M., Bower, D.J., Cannon, J., 2016. Ocean basin evolution and global-scale plate reorganization events since Pangea breakup. Annu. Rev. Earth Planet. Sci. 44, 107–138.
Nelson, R.W., Bartram, J.A., Christie, M.H., 1990. Hidden Valley gold-silver deposit. In: Hughes, F.E. (Ed.), Geology of the mineral deposits of Australia and Papua New Guinea. The Australasian Institute of Mining and Metallurgy, Melbourne, pp. 1773–1776.
Niespolo, E.M., Rutte, D., Deino, A.L., Renne, P.R., 2016. Intercalibration and age of the Alder Creek sanidine $^{40}Ar/^{39}Ar$ standard. Quat. Geochronol.
Ott, B., Mann, P., 2015. Late Miocene to Recent formation of the Aure-Moresby fold-thrust belt and foreland basin as a consequence of Woodlark microplate rotation, Papua New Guinea. Geochem., Geophys., Geosyst. https://doi.org/10.1002/2014GC005668.
Page, R.W., 1976. Geochronology of igneous and metamorphic rocks in the New Guinea Highlands. Bureau of Mineral Resources, Geology and Geophysics Bulletin 162. Australian Government Publishing Service, Canberra.
Page, R.W., McDougall, I., 1972a. Geochronology of the Panguna porphyry copper deposit, Bougainville Island, New Guinea. Econ. Geol. 67, 1065–1074.
Page, R.W., McDougall, I., 1972b. Ages of mineralization of gold and porphyry copper deposits in the New Guinea Highlands. Econ. Geol. 67, 1034–1048.
Petterson, M.G., Babbs, T., Neal, C.R., Mahoney, J.J., Saunders, A.D., Duncan, R.A., Tolia, D., Magu, R., Qopoto, C., Mahoa, H., Natogga, D., 1999. Geological-tectonic framework of Solomon Islands, SW Pacific: crustal accretion and growth with an intra-oceanic setting. Tectonophysics 301, 35–60.
Petterson, M.G., Neal, C.R., Mahoney, J.J., Kroenke, L.W., Saunders, A.D., Babbs, T.L., Duncan, R.A., Tolia, D., McGrail, B., 1997. Structure and deformation of north and central Malaita, Solomon Islands: tectonic implications for the Ontong Java Plateau-Solomon arc collision, and for the fate of oceanic plateaus. Tectonophysics 283, 1–33.
Phinney, E.J., Mann, P., Coffin, M.F., Shipley, T.H., 2004. Sequence stratigraphy, structural style, and age of deformation of the Malaita accretionary prism (Solomon arc-

Ontong Java Plateau convergent zone). Tectonophysics 389, 221–246.
Pigram, C.J., Davies, H.L., 1987. Terranes and the accretion history of the New Guinea Orogen. BMR J. Aust. Geol. Geophys. 10, 193–211.
Rapp, R.P., Watson, E.B., 1995. Dehydration melting of metabasalt at 8–32 kbar: Implications for continental growth and crust-mantle recycling. J. Petrol. 36, 891–931.
Richards, J.P., 2003. Tectono-magmatic precursors for porphyry Cu-(Mo-Au) deposit formation. Econ. Geol. 98, 1515–1533.
Richards, J.P., 2011. High Sr/Y arc magmas and porphyry Cu ± Mo ± Au deposits: just add water. Econ. Geol. 106, 1075–1081.
Richards, J.P., 2013. Giant ore deposits formed by optimal alignments and combinations of geological processes. Nat. Geosci. 6, 911–916.
Richards, J.P., Kerrich, R., 2007. Adakite-like rocks: Their diverse origins and questionable role in metallogenesis. Econ. Geol. 102, 537–576.
Richards, J.P., Ledlie, I., 1993. Alkalic intrusive rocks associated with the Mount Kare gold deposit, Papua New Guinea; comparison with the Porgera intrusive complex. Econ. Geol. 88, 755–781.
Richards, J.P., McDougall, I., 1990. Geochronology of the Porgera gold deposit, Papua New Guinea: Resolving the effects of excess argon on K-Ar and 40Ar/39Ar age estimates for magmatism and mineralization. Geochim. Cosmochim. Acta 54, 1397–1415.
Richards, S.W., Holm, R.J., 2013. Tectonic preconditioning and the formation of giant porphyry deposits. Econ. Geol. Spec. Publ. 17, 265–275.
Rohrbach, A., Schuth, S., Ballhaus, C., Münker, C., Matveev, S., Qopoto, C., 2005. Petrological constraints on the origin of arc picrites, New Georgia Group, Solomon Islands. Contrib. Miner. Petrol. 149, 685–698.
Rosenbaum, G., Giles, D., Saxon, M., Betts, P.G., Weinberg, R.F., Duboz, C., 2005. Subduction of the Nazca Ridge and the Inca Plateau: Insights into the formation of ore deposits in Peru. Earth Planet. Sci. Lett. 239, 18–32.
Rosenbaum, G., Mo, W., 2011. Tectonic and magmatic responses to the subduction of high bathymetric relief. Gondwana Res. 19, 571–582.
Rytuba, J.J., McKee, E.H., Cox, D., 1993. Geochronology and geochemistry of the Ladolam gold deposit, Lihir Island, and gold deposits and volcanoes of Tabar and Tatau, Papua New Guinea. USGS Bulletin 2039, 119–126.
Schellart, W.P., Lister, G.S., Toy, V.G., 2006. A Late Cretaceous and Cenozoic reconstruction of the southwest Pacific region: Tectonics controlled by subduction and slab rollback processes. Earth Sci. Rev. 76, 191–233.
Schellart, W.P., Spakman, W., 2015. Australian plate motion and topography linked to fossil New Guinea slab below Lake Eyre. Earth Planet. Sci. Lett. 421, 107–116.
Schuth, S., Münker, C., König, S., Qopoto, C., Basi, S., Garbe-Schönberg, D., Ballhaus, C., 2009. Petrogenesis of lavas along the Solomon Island arc, SW Pacific: Coupling of compositional variations and subduction zone geometry. J. Petrol. 50, 781–811.
Sen, C., Dunn, T., 1994. Dehydration melting of a basaltic composition amphibolite at 1.5 and 2.0 GPa: Implications for the origin of adakites. Contrib. Miner. Petrol. 117, 394–409.
Seton, M., Mortimer, N., Williams, S., Quilty, P., Gans, P., Meffre, S., Micklethwaite, S., Zahirovic, S., Moore, J., Matthews, K.J., 2016. Melanesian back-arc basin and arc development: constraints from the eastern Coral Sea. Gondwana Res. 39, 77–95.
Seton, M., Müller, R.D., Zahirovic, S., Gaina, C., Torsvik, T., Shephard, G., Talsma, A., Gurnis, M., Turner, M., Maus, S., Chandler, M., 2012. Global continental and ocean basin reconstructions since 200 Ma. Earth Sci. Rev. 113, 212–270.
Sillitoe, R.H., 1989. Gold deposits in western Pacific island arcs; the magmatic connection. Econ. Geol. Monogr. 6, 274–291.
Sillitoe, R.H., 2008. Major gold deposits and belts of the North and South American Cordillera: distribution, tectonomagmatic setting, and metallogenic considerations. Econ. Geol. 103, 663–687.
Sillitoe, R.H., 2010. Porphyry copper systems. Econ. Geol. 105, 3–41.
Singer, D.A., Berger, V.I., Moring, B.C., 2008. Porphyry copper deposits of the world: Database and grade and tonnage models. U.S., Geological Survey Open-File Report 2008-1155.
Smith, I.E.M., 1976. Volcanic rocks from southeastern Papua: The Evolution of volcanism at a plate boundary (Unpublished. PhD Thesis. Australian National University, Canberra, pp. p. 298)..
Smith, I.E., 1982. Volcanic evolution in eastern Papua. Tectonophysics 87, 315–333.
Smith, D.J., Jenkin, G.R.T., Naden, J., Boyce, A.J., Petterson, M.G., Toba, T., Darling, W.G., Taylor, H., Millar, I.L., 2010. Anomalous alkaline sulphate fluids produced in a magmatic hydrothermal system—Savo, Solomon Islands. Chem. Geol. 275, 35–49.
Smith, D.J., Jenkin, G.R.T., Petterson, M.G., Naden, J., Fielder, S., Toba, T., Chenery, S.R.N., 2011. Unusual mixed silica–carbonate deposits from magmatic–hydrothermal hot springs, Savo, Solomon Islands. J. Geol. Soc. 168, 1297–1310.
Smith, D., Petterson, M., Saunders, A., Millar, I.L., Jenkin, G.R.T., Toba, T., Naden, J., Cook, J.M., 2009. The petrogenesis of sodic island arc magmas at Savo Volcano, Solomon Islands. Contrib. Miner. Petrol. 158, 785–801.
Stracke, A., Hegner, E., 1998. Rifting-related volcanism in an oceanic post-collisional setting: the Tabar-Lihir-Tanga-Feni (TLTF) island chain, Papua New Guinea. Lithos 45, 545–560.
Struckmeyer, H.I.M., Yeung, M., Pigram, C.J., 1993. Mesozoic to Cainozoic plate tectonic palaeographic evolution of the New Guinea region. In: Carman, G.J., Carman, Z. (Eds.), Petroleum Exploration in Papua New Guinea. Proceedings of the Second PNG Petroleum Convention, Port Moresby, pp. 261–290.
Swiridiuk, P., 1998. Exploring the Solomon Islands with airborne geophysics. Explor. Geophys. 29, 620–625.
Taira, A., Mann, P., Rahardiawan, R., 2004. Incipient subduction of the Ontong Java Plateau along the North Solomon trench. Tectonophysics 389, 247–266.
Tapster, S., Condon, D.J., Naden, J., Noble, S.R., Petterson, M.G., Roberts, N.M.W., Saunders, A.D., Smith, D.J., 2016. Rapid thermal rejuvenation of high-crystallinity magma linked to porphyry copper deposit formation; evidence from the Koloula Porphyry Prospect, Solomon Islands. Earth Planet. Sci. Lett. 442, 206–217.
Tapster, S., Petterson, M.G, Jenkin, G.R.T, Saunders, A.D. Smith, D.J, Naden, J., 2011. Preliminary petrogenetic and geodynamic controls on magmatic-hydrothermal Cu and Au mineralisation of Guadalcanal, Solomon Islands. In Barra, F. et al. (Eds) LET'S TALK ORE DEPOSITS. Proceedings of the 11th Biennial SGA Meeting, Antofagasta, Chile, 2, 577-579.
Tapster, S., Roberts, N.M.W., Petterson, M.G., Saunders, A.D., Naden, J., 2014. From continent to intra-oceanic arc: Zircon xenocrysts record the crustal evolution of the Solomon island arc. Geology 42, 1087–1090.
Taylor, B., 1979. Bismarck Sea: Evolution of a back-arc basin. Geology 7, 171–174.
Taylor, B., Goodliffe, A.M., Martinez, F., 1999. How continents break up: Insights from Papua New Guinea. J. Geophys. Res. 104, 7497–7512.
Taylor, B., Goodliffe, A., Martinez, F., Hey, R., 1995. Continental rifting and initial seafloor spreading in the Woodlark basin. Nature 374, 534–537.
Thomas, R.J., Spencer, C., Bushi, A.M., Baglow, N., Boniface, N., de Kock, G., Horstwood, M.S., Hollick, L., Jacobs, J., Kajara, S., Kamihanda, G., 2016. Geochronology of the central Tanzania Craton and its southern and eastern orogenic margins. Precambr. Res. 277, 47–67.
Titley, S.R., 1978. Geologic history, hypogene features, and processes of secondary sulfide enrichment at the Plesyumi copper prospect, New Britain, Papua New Guinea. Econ. Geol. 73, 768–784.
Turner, C.C., Ridgway, J., 1982. Tholeiitic, calc-alkaline and (?) alkaline igneous rocks of the Shortland islands, Solomon Islands. Tectonophysics 87, 335–354.
Van Donge, M., Weinberg, R.F., Tomkins, A.G., 2010. REE-Y, Ti, and P remobilization in magmatic rocks by hydrothermal alteration during Cu-Au deposit formation. Econ. Geol. 105, 763–776.
van Dongen, M., Weinberg, R.F., Tomkins, A.G., Armstrong, R.A., Woodhead, J.D., 2010. Recycling of Proterozoic crust in Pleistocene juvenile magma and rapid formation of the Ok Tedi porphyry Cu-Au deposit, Papua New Guinea. Lithos 114, 282–292.
Wallace, L.M., Ellis, S., Little, T., Tregoning, P., Palmer, N., Rosa, R., Stanaway, R., Oa, J., Nidkombu, E., Kwazi, J., 2014. Continental breakup and UHP rock exhumation in action: GPS results from the Woodlark Rift, Papua New Guinea. Geochem. Geophys. Geosyst. 15, 4267–4290.
Wallace, L.M., Stevens, C., Silver, E., McCaffrey, R., Loratung, W., Hasiata, S., Stanaway, R., Curley, R., Rosa, R., Taugaloidi, J., 2004. GPS and seismological constraints on active tectonics and arc-continent collision in Papua New Guinea: Implications for mechanics of microplate rotations in a plate boundary zone. J. Geophys. Res. 19, B05404. https://doi.org/10.1029/2003JB002481.
Webb, L.E., Baldwin, S.L., Fitzgerald, P.G., 2014. The Early-Middle Miocene subduction complex of the Louisiade Archipelago, southern margin of the Woodlark Rift. Geochem. Geophys. Geosyst. 15, 4024–4046.
Weiland, R.J., 1999. Emplacement of the Irian Ophiolite and unroofing of the Ruffaer Metamorphic Belt of Irian Jaya, Indonesia. PhD thesis. University of Texas at, Austin, pp. 526 pp..
Wells, R.E., 1989. Origin of the oceanic basalt basement of the Solomon Islands arc and its relationship to the Ontong Java Plateau – insights from Cenozoic plate motion models. Tectonophysics 165, 219–235.
Whalen, J.B., Britten, R.M., McDougall, I., 1982. Geochronology and geochemistry of the Frieda River prospect area, Papua New Guinea. Econ. Geol. 77, 592–616.
Wilcox, R.E., Harding, T.P., Seely, D.R., 1973. Basic wrench tectonics. Am. Assoc. Pet. Geol. 57, 74–96.
Woodhead, J.D., Eggins, S.M., Johnson, R.W., 1998. Magma genesis in the New Britain island arc: further insights into melting and mass transfer processes. J. Petrol. 39, 1641–1668.
Woodhead, J., Hergt, J., Sandiford, M., Johnson, W., 2010. The big crunch: Physical and chemical expressions of arc/continent collision in the Western Bismarck arc. J. Volcanol. Geoth. Res. 190, 11–24.